SANDIA REPORT

SAND2010-6317
Unlimited Release
Printed September 2010

Peridynamics as a Rigorous Coarse-Graining of Atomistics for Multiscale Materials Design

John A. Aidun (PM), James R. Kamm, Richard B. Lehoucq (PI), Michael L. Parks, Mark P. Sears and Stewart A. Silling

Prepared by
Sandia National Laboratories
Albuquerque, New Mexico 87185 and Livermore, California 94550

Sandia National Laboratories is a multi-program laboratory managed and operated by Sandia Corporation, a wholly owned subsidiary of Lockheed Martin Corporation, for the U.S. Department of Energy's National Nuclear Security Administration under contract DE-AC04-94AL85000.

Approved for public release; further dissemination unlimited.

Sandia National Laboratories

Issued by Sandia National Laboratories, operated for the United States Department of Energy by Sandia Corporation.

NOTICE: This report was prepared as an account of work sponsored by an agency of the United States Government. Neither the United States Government, nor any agency thereof, nor any of their employees, nor any of their contractors, subcontractors, or their employees, make any warranty, express or implied, or assume any legal liability or responsibility for the accuracy, completeness, or usefulness of any information, apparatus, product, or process disclosed, or represent that its use would not infringe privately owned rights. Reference herein to any specific commercial product, process, or service by trade name, trademark, manufacturer, or otherwise, does not necessarily constitute or imply its endorsement, recommendation, or favoring by the United States Government, any agency thereof, or any of their contractors or subcontractors. The views and opinions expressed herein do not necessarily state or reflect those of the United States Government, any agency thereof, or any of their contractors.

Printed in the United States of America. This report has been reproduced directly from the best available copy.

Available to DOE and DOE contractors from
U.S. Department of Energy
Office of Scientific and Technical Information
P.O. Box 62
Oak Ridge, TN 37831

Telephone: (865) 576-8401
Facsimile: (865) 576-5728
E-Mail: reports@adonis.osti.gov
Online ordering: http://www.osti.gov/bridge

Available to the public from
U.S. Department of Commerce
National Technical Information Service
5285 Port Royal Rd
Springfield, VA 22161

Telephone: (800) 553-6847
Facsimile: (703) 605-6900
E-Mail: orders@ntis.fedworld.gov
Online ordering: http://www.ntis.gov/help/ordermethods.asp?loc=7-4-0#online

2010-6317
Unlimited Release
Printed September 2010

Peridynamics as a Rigorous Coarse-Graining of Atomistics for Multiscale Materials Design

John A. Aidun[2] (PM), James R. Kamm[3], Richard B. Lehoucq[1](PI), Michael L. Parks[1], Mark P. Sears[2], Stewart A. Silling[2]

[1] Applied Mathematics and Applications (1414)
[2] Multiscale Dynamic Material Modeling (1435)
[3] Computational Shock & Multiphysics (1431)

Sandia National Laboratories
P.O. Box 5800
Albuquerque, NM 87185-1320

Abstract

This report summarizes activities undertaken during FY08-FY10 for the LDRD *Peridynamics as a Rigorous Coarse-Graining of Atomistics for Multiscale Materials Design.* The goal of our project was to develop a coarse-graining of finite temperature molecular dynamics (MD) that successfully transitions from statistical mechanics to continuum mechanics.

Contents

1 Peridynamics as a Rigorous Coarse-Graining of Atomistics for Multiscale Materials Design **11**

Project Purpose 11

Accomplishments 11

Published papers 12

Organization of the report 13

2 A Peridynamics-Inspired Approach to Nonlocal Advection **15**

Introduction 15

The advection equation 15

Non-local advection 16

Previous approaches to non-local advection 16

Non-local advection: a new formulation 16

An approach to solving the non-local advection equation 17

Open issues in non-local advection equation 18

Regularization of non-local advection 18

Shocks in non-local advection 19

Entropy in non-local advection 19

Non-local Burgers Equation 19

Conclusions 20

3 Peridynamics with LAMMPS: A User Guide **21**

Introduction 21

Quick Start Guide 21

Typographical Conventions 21

Getting Started . . . 22
Building the Peridynamic Module within LAMMPS . . . 22
Input Script Basics . . . 22
Peridynamic Model of a Continuum . . . 24
Basic Notation . . . 24
Linear Peridynamic Solid (LPS) Model . . . 25
Prototype Microelastic Brittle (PMB) Model . . . 26
Damage . . . 27
Discrete Peridynamic Model and LAMMPS Implementation . . . 28
Spatial Discretization . . . 28
Short-Range Forces . . . 28
Modification to the Particle Volume . . . 29
Temporal Discretization . . . 30
Breaking Bonds . . . 30
LPS Pseudocode . . . 30
PMB Pseudocode . . . 30
Damage . . . 30
Visualizing Simulation Results . . . 33
Pitfalls . . . 34
Bugs . . . 35
Modifying and Extending the Peridynamic Module . . . 35
A Numerical Example . . . 35
Problem Description and Setup . . . 35
The Projectile . . . 36
Writing the LAMMPS Input File . . . 36
Numerical Results and Discussion . . . 37

4 The mapping from particle mechanics to continuum mechanics 39

Introduction . . . 39

Continuum mechanics. 41
Mass density. 42
Momentum density. 42
Total and internal energy densities. 42
Particle mechanics. 43
Hamiltonian particle mechanics. 43
Conservation laws. 43
Galilean invariance. 44
Decomposition of the force. 44
Further discussion about reflection invariance. 48
Microscopic densities. 49
Observed densities. 49
Conservation of mass. 50
Conservation of momentum. 52
Hardy's method. 53
The Fourier method. 54
Conservation of angular momentum. 54
Conservation of energy. 55
Summary. 60
Conclusions. 61

References **65**

Distribution **68**

List of Figures

3.1 Diagram showing horizon of a particular particle, demonstrating that the volume associated with particles near the boundary of the horizon is not completely contained within the horizon. 29

3.2 Target during (a) and after (b,c) impact. 38

List of Tables

3.1 Notational conventions. 22

Chapter 1

Peridynamics as a Rigorous Coarse-Graining of Atomistics for Multiscale Materials Design

Project Purpose

The goal of our project is to develop a coarse-graining of finite temperature molecular dynamics (MD) that successfully transitions from statistical mechanics to continuum mechanics. Our coarse-graining overcomes the intrinsic limitation of coupling atomistics with classical continuum mechanics via the FEM (finite element method), SPH (smoothed particle hydrodynamics), or MPM (material point method); namely, that classical continuum mechanics assumes a local force interaction that is incompatible with the nonlocal force model of atomistic methods. Therefore FEM, SPH, and MPM inherit this limitation. This seemingly innocuous dichotomy has far reaching consequences; for example, classical continuum mechanics cannot resolve the short wavelength behavior associated with atomistics. Other consequences include spurious forces, invalid phonon dispersion relationships, and irreconcilable descriptions/treatments of temperature. We propose a statistically based coarse-graining of atomistics via peridynamics and so develop a first of a kind mesoscopic capability to enable consistent, thermodynamically sound, atomistic-to-continuum (AtC) multiscale material simulation. Peridynamics (PD) is a microcontinuum theory that assumes nonlocal forces for describing long-range material interaction. The force interactions occurring at finite distances are naturally accounted for in PD. Moreover, PDs nonlocal force model is entirely consistent with those used by atomistics methods, in stark contrast to classical continuum mechanics. Hence, PD can be employed for mesoscopic phenomena that are beyond the realms of classical continuum mechanics and atomistic simulations, e.g., molecular dynamics and density functional theory (DFT). The latter two atomistic techniques are handicapped by the onerous length and time scales associated with simulating mesoscopic materials. Simulating such mesoscopic materials is likely to require, and greatly benefit from multiscale simulations coupling DFT, MD, PD, and explicit transient dynamic finite element methods FEM (e.g., Presto). The proposed work fills the gap needed to enable multiscale materials simulations.

Accomplishments

The project goal of establishing the theoretical groundwork for coarse-graining MD into peridynamics was accomplished. This project accomplishment is documented in three related approaches

and in three Sandia technical reports. The first approach derives the peridynamic balance of linear momentum from the principles of statistical mechanics. The second approach upscales molecular dynamics into a high order gradient theory, and exploits a relationship between peridynamics and a high order gradient theory. The third approach represents an interatomic multibody potential as a peridynamic material, and then smoothes the resulting heterogeneous peridynamic material model. In recognition of these accomplishments, the project team received a Sandia employee recognition award. The three coarse-graining approaches described above are synergistic. The first approach, though of significant theoretical value, does not immediately lead to an expedient computational scheme. An important conclusion is that the path from classical statistical to classical continuum mechanics traverses the nonlocal continuum theory of peridynamics. A consequence is that peridynamics can augment, or replace, MD, and AtC coupling can be replaced by PtC coupling (peridynamics to classical continuum mechanics). The second approach is a practical application justifying the contention of the first approach that molecular dynamics can be coarse-grained into peridynamics. In contrast to classical continuum mechanics, peridynamics does capture the short-wavelength behavior associated with molecular dynamics without the need to assume the existence of higher-order derivatives associated with a high-order gradient theory. The third approach represents a sophisticated scheme for generating peridynamic material models by coarse-graining multibody interatomic potentials at the continuum level. The third approach represents a sophisticated scheme for generating peridynamic material models by coarse-graining multibody interatomic potentials at the continuum level.

Published papers

1. *Peridynamics as an Upscaling of Molecular Dynamics*, P. Seleson, M. L. Parks, M. Gunzburger, and R. B. Lehoucq, **Multiscale Modeling and Simulation**, 8, pp. 204-227, 2009, DOI:10.1137/09074807X.

2. *Implementing Peridynamics within a Molecular Dynamics Code*, M. L. Parks, R. B. Lehoucq, S. J. Plimpton, and S. A. Silling, **Computer Physics Communications**, 179, pp. 777-783, 2008, DOI:10.1016/j.cpc.2008.06.011.

3. *Peridynamic Theory of Solid Mechanics*, S. A. Silling and R. B. Lehoucq, **Advances In Applied Mechanics**, 44, pp. 73–169, 2010, DOI: 10.1016/S0065-2156(10)44002-8.

4. *Translation of Walter Nolls "Derivation of the Fundamental Equations of Continuum Thermodynamics from Statistical Mechanics"* R. B. Lehoucq and A. Von Lilienfeld-Toal, **Journal of Elasticity**, 100, pp. 5-24, 2010, DOI:10.1007/s10659-010-9246-9.

5. *Linearized theory of peridynamic states*, S. A. Silling, **Journal of Elasticity**, 99, 85-111, 2010, DOI:10.1007/s10659-009-9234-0.

6. *Mathematical analysis for the peridynamic nonlocal continuum theory*, Q. Du and K. Zhou, **ESAIM: Mathematical Modelling and Numerical Analysis**, DOI:10.1051/m2an/2010040.

7. *Mathematical and Numerical Analysis of Linear Peridynamic Models with Nonlocal Boundary Conditions*, Q. Du and K. Zhou, Accepted for publication in the **SIAM Journal of Numerical Analysis**, 2010.

8. *On the Role of the Influence Function in the Peridynamic Theory*, P. Seleson and M. L. Parks, Accepted for publication in the **International Journal for Multiscale Computational Engineering** 2010.

9. *A coarsening method for linear peridynamics*, S. A. Silling, Accepted for publication in the **International Journal for Multiscale Computational Engineering** 2010.

Organization of the report

Chapter 2

A Peridynamics-Inspired Approach to Nonlocal Advection

Introduction

This report describes an approach to nonlocal, nonlinear advection in one dimension. This development extends the usual pointwise concepts to account for nonlocal contributions to the fluxes. The spatially nonlocal operators we consider do not involve local derivatives. Instead, these nonlocal expressions involve integral operators that, in the appropriate limit, reduce to the familiar local equations. These ideas are motivated by the fundamental approach upon which peridynamics [51] is built. Unlike the usual peridynamics equations for, say, elastic material response, we specialize to nonlocal, nonlinear advection equations. We restrict our attention to explore model equations that capture the fundamental character of *nonlocal* shock wave phenomena. Our ultimate goal is to incorporate a consistent, defensible approach to nonlocal shock physics into the existing peridynamics framework. As a first step, we develop a nonlocal, inviscid Burgers equation as an intrinsically nonlinear example of these ideas.

The advection equation

The concept of advection and use of advection equations is widespread in applied mathematics and fundamental in physics. Such equations provide a simple and extensible basis with which to model conservation equations, which lie at the foundation of many physics principles. The essential representation of this concept is contained in a balance equation between the time rate-of-change of some quantity u and the corresponding spatial divergence of some function f—the flux function—of that same quantity:

$$u_t + \operatorname{div} f(u) = 0\,. \tag{2.0.1}$$

Unless stated otherwise, we assume that there is no external source or sink, so that the RHS of (2.0.1) is zero. We consider exclusively the one-dimensional case, so that the advection equation reduces to

$$u_t + f_x(u) = 0 \quad \text{or} \quad u_t + f'(u)\,u_x = 0\,, \tag{2.0.2}$$

where the second equation holds for f differentiable in u and u differentiable in x. In the simplest case, the flux function is proportional to the field itself, which leads to the linear one-way wave equation,

$$u_t + c\,u_x = 0\,, \quad c \in \mathbb{R}\,. \tag{2.0.3}$$

This equation possesses the traveling wave solution, $u(x,t) = g(x - ct)$, where $g(x) = f(x, t = 0)$ is the initial condition; for $c > 0$, this represents uniform translation of the initial wave profile to the right at constant speed c. The simplest nonlinear case is given by a flux function quadratic in u, yielding the well-known inviscid Burgers equation,

$$u_t + \left(u^2/2\right)_x = 0 \quad \text{or} \quad u_t + u\, u_x = 0\,, \tag{2.0.4}$$

where, again, the second equation holds if u is differentiable in x. This equation is an elementary yet powerful model for many shock phenomena, as it has a convex flux function, $f(u) = u^2/2$, leads to the development of shocks in finite time for smooth-but-nontrivial initial conditions, and forms a basis for exploring important concepts, such as entropy. The fundamental ideas underlying local advection, embodied in such equations, have been developed by numerous researchers in countless applications, and have been examined theoretically, analytically, and computationally.

Non-local advection

The exhaustive study that has been conducted of local advection has not been applied to *nonlocal* advection. Here, we briefly mention other approaches and describe our new work.

Previous approaches to non-local advection

The literature contain instances of what may be generally termed "nonlocal advection" (sometimes referred to as "nonlocal convection"). Assuming that the time derivative is treated locally (i.e., as the usual partial derivative $\partial/\partial t$), there are two main aspects of the general advection equation for which nonlocal extensions have been examined: (i) nonlocal f, nonlocal $f_x(u)$ in (2.0.2a), or nonlocal $f'(u)$ in (2.0.2b), and (ii) nonlocal regularizations, i.e., "small" nonlocal terms replacing the zero on the RHS of the equality in both equations in (2.0.2). The first of these approaches was considered, e.g., in [6, 9, 14, 38, 56, 66], while the second category of nonlocalizations includes some of the above cited works, as well as, e.g., [1, 2, 4, 7, 11, 15, 16, 19, 28, 27, 36, 37, 56, 49, 63, 64]. A focus of many of these works is on nonlocal generalizations of Burgers equation. Moreover, in most of these studies, assumptions are made regarding the particular form of the nonlocality; for example, in [4] and [9], the Hilbert transform of u is used to model nonlocal behavior. Such assumptions are perfectly sensible for modeling specific physics, but they are not general in nature.

Non-local advection: a new formulation

The approaches of the previous section impose some specific assumptions on the nonlocality, either in the advective operator or in the regularization term. Motivated by peridynamics, we consider a more general case and posit the following integro-differential equation:

$$\begin{aligned} u_t(x,t) + \int_{\mathbb{R}} dy\, \psi\left(\frac{u(y,t) + u(x,t)}{2}\right)\phi_a(y,x) &= 0 \qquad (x,t) \in \mathbb{R} \times (0,\infty)\,, \\ u(x,0) &= g(x) \qquad\qquad x \in \mathbb{R}\,, \end{aligned} \tag{2.0.5}$$

where the kernel[1] is antisymmetric in its arguments: $\phi_a(y,x) = -\phi_a(x,y)$. We claim that this equation represents a general nonlocal, nonlinear conservation law for advection. To see that this is the case, consider the special case in which the kernel is the derivative of the Dirac delta distribution:

$$\phi_a(y,x) \equiv -\frac{d}{dy}\delta(y-x)\,, \tag{2.0.6}$$

and assume further that ψ, u, and u_x decay sufficiently fast to zero as their arguments approach infinity. Integration by parts of (2.0.5) implies that

$$\begin{aligned}\int_{\mathbb{R}} dy\,\psi\left(\frac{u(y,t)+u(x,t)}{2}\right)\phi_a(y,x) &= -\left[\psi\left(\frac{u(y,t)+u(x,t)}{2}\right)\delta(y-x)\right]\Bigg|_{y=-\infty}^{y=\infty} \\ &\quad + \int_{\mathbb{R}} dy\,\psi_y\left(\frac{u(y,t)+u(x,t)}{2}\right)\delta(y-x) \;=\; \psi_x\big(u(x,t)\big)\,. \end{aligned} \tag{2.0.7}$$

Comparing this result with (2.0.2), we immediately identify ψ with the corresponding *local* flux function f and see that, for the particular kernel given in (2.0.6), (2.0.5) reduces to its local counterpart:

$$\begin{aligned} u_t + f_x(u) &= 0 \qquad (x,t)\in\mathbb{R}\times(0,\infty)\,, \\ u(x,0) &= g(x) \qquad\qquad\qquad x\in\mathbb{R}\,. \end{aligned} \tag{2.0.8}$$

We gain more insight into the nature of (2.0.5) by applying Noll's Lemma I [44, 33], which, under certain boundedness and smoothness assumptions, gives an explicit expression for flux function f for (2.0.5):

$$f\big(u(x,t)\big) = -\frac{1}{2}\int_{\mathbb{R}} dz \int_0^1 d\lambda\,\psi\left(\frac{u(x-(1-\lambda)z,t)+u(x+\lambda z,t)}{2}\right) z\,\phi_a(x-(1-\lambda)z, x+\lambda z) \tag{2.0.9a}$$

such that

$$f_x\big(u(x,t)\big) = \int_{\mathbb{R}} dy\,\psi\left(\frac{u(y,t)+u(x,t)}{2}\right)\phi_a(y,x)\,. \tag{2.0.9b}$$

This result confirms that (2.0.5) can be written in the form of (2.0.2) with the flux function given by (2.0.9a).

An approach to solving the non-local advection equation

Consider now (2.0.5) in the form given by the second equation in (2.0.2), together with the flux function relations (2.0.9a),(2.0.9b). Along the characteristic curves, given by the ODEs

$$\frac{dx}{dt} = f'(u)\,, \quad x(0) = x_0\,, \tag{2.0.10}$$

where x_0 labels the initial point $(x,t) = (x_0, 0)$, (2.0.2) can be written as the perfect derivative

$$\frac{du}{dt} = 0\,, \quad u(0) = g(x_0)\,. \tag{2.0.11}$$

[1]The kernel of the integral is called the micromodulus in the peridynamics literature.

Together, (2.0.10) and (2.0.11) imply that the solution to (2.0.5) satisfies the implicit equation

$$u(x,t) = g\big(x - t\, f'(u(x,t))\big) \quad \Rightarrow \quad G(u(x,t)) \equiv g\big(x - t\, f'(u(x,t))\big) - u(x,t) = 0\,. \tag{2.0.12}$$

From the chain rule applied to the flux function f, we have the following relation

$$f_x(u(x,t)) = f_u(u(x,t)) \cdot u_x(x,t) \quad \Rightarrow \quad f_u(u(x,t)) \equiv f'(u(x,t)) = f_x(u(x,t))/u_x(x,t)\,. \tag{2.0.13}$$

In (2.0.12), (2.0.13), and (2.0.9b) we have key components used in a numerical algorithm with which to obtain solutions to (2.0.5) as the roots of the function G in (2.0.12). This is the same approach that can be applied to find solutions to the local advection equation. Unlike the local case, where this solution procedure leads to a series of explicit root-solves for $G(u) = 0$ at each (x,t), in the nonlocal case the solution for $G(u) = 0$ leads to an inherently *implicit* problem, as the values of $u(x,t)$ at all values of x are coupled through the nonlocal flux, i.e., the second addend in (2.0.5).

Open issues in non-local advection equation

Suggested by analysis of local advection equations, there are numerous open issues to be addressed for the nonlocal advection equation given in (2.0.5). We list a few of the most important topics here.

Regularization of non-local advection

The regularization of inviscid advection equations (such as (2.0.2)) plays an important role in the associated physics and mathematics. Here, by the term *regularization* we mean the modification of the otherwise-zero RHS of the conservation law with terms that are small relative to the scale of the solution. Inspired by the work of Gunzberger and Lehoucq [21] and informed by the work of Ignat and Rossi [25], we propose a regularization of the (inviscid) nonlocal advection equation (2.0.5) of the following form:

$$\begin{aligned} u_t(x,t) + \int_{\mathbb{R}} dy\, \psi\!\left(\frac{u(y,t)+u(x,t)}{2}\right)\phi_a(y,x) &= \epsilon \int_{\mathbb{R}} dy\, \big(u(y,t) - u(x,t)\big)\phi_s(y,x) \quad (x,t) \in \mathbb{R}\times(0,\infty)\,, \\ u(x,0) &= g(x) \qquad\qquad\qquad\qquad\qquad\qquad\qquad\qquad x \in \mathbb{R}\,, \end{aligned} \tag{2.0.14}$$

where the kernel ϕ_s is symmetric in its arguments: $\phi_s(y,x) = \phi_s(x,y)$. We claim that this equation represents a general nonlocal, nonlinear conservation law for advection. Using arguments similar to those presented in §2, with the particular symmetric kernel

$$\phi_s(y,x) \equiv -\frac{d^2}{dy^2}\delta(y-x)\,, \tag{2.0.15}$$

one can show that

$$\int_{\mathbb{R}} dy\, \big(u(y,t) - u(x,t)\big)\psi_s(y,x)y = u_{xx}(x,t)\,. \tag{2.0.16}$$

Thus, the regularized nonlocal equation (2.0.14), for ϕ_s as in (2.0.15) and ϕ_a as in (2.0.6), reduces to the viscous conservation law

$$u_t + f_x(u) = \epsilon\, u_{xx}\,. \tag{2.0.17}$$

While shock waves are often idealized as inviscid structures, it is only through the proper regularization of the governing conservation equations, associated with vanishing viscosity, that shock formation and propagation can be properly understood. The form of the equation given (2.0.14) forms the nonlocal approach to a regularized (viscous) nonlocal conservation law consistent with the (inviscid) nonlocal advection equation given in (2.0.5).

Shocks in non-local advection

There are innumerable references on this shock waves, among them being [60, 42]. Burgers equation, as discussed, e.g., in [65, 34, 35], provides a model equation with which to examine many of the key issues related to basic shock physics. We propose to study the nonlocal Burgers equation, introduced in (2.0.4), for exactly this reason: to understand the fundamental aspects of idealized, nonlocal shock physics. This remains an as-yet unrealized aspect of our work.

Entropy in non-local advection

The concept of entropy has proved crucial in both the physical understanding of and computational approach to shock waves. Understanding the physics of entropy production through shock waves was a seminal finding in 20th century continuum mechanics. The corresponding mathematical understanding has developed over the last ∼50 years and is well codified for 1D shocks [13, 18, 32, 57, 61]. In particular, the concept of the entropy-flux/entropy-function pair (see the previous references) provides an instructional picture of the shock selection mechanism for local equations. We posit that a very similar analysis for the nonlocal advection equation may hold, although the analysis is likely more complicated in the nonlocal case. It is exactly this type of careful analysis that will provide the basis of rigorous understanding of nonlocal shock propagation.

Non-local Burgers Equation

Using the approach to nonlocal advection discussed in previous section, we propose a new nonlocal (inviscid) Burgers equation of the form

$$u_t(x,t) = \int_{-\infty}^{\infty} dy\, \psi\left(\frac{u(y,t)+u(x,t)}{2}\right) \phi_a(y,x)\,, \tag{2.0.18}$$

where $\psi(u) = u^2/2$ is the usual (i.e., local) Burgers flux function and, following the discussion after (2.0.5), the kernel ϕ_a is an antisymmetric function of its arguments. Following the procedure of §2, setting the kernel to the generalized function $\phi_a(y,x) = \partial_y(\delta(y-x))$, one finds that (2.0.18) reduces to the local Burgers equation (2.0.4).

The corresponding nonlocal viscous Burgers equation corresponds to (2.0.14) with the flux function given in the preceding paragraph. One important aspect of the viscous Burgers equation is the existence of a closed-form solution (see, e.g., [65]); another is the ability to examine the vanishing viscosity behavior (i.e., as $\epsilon \to 0^+$) of the solution. A tantalizing open question is whether a similar solution obtains for the nonlocal viscous Burgers equation, perhaps through a nonlocal analogue of the Cole-Hopf procedure [12, 24]. Such a solution would be desirable as a

definitive benchmark against which to evaluate general numerical methods for solving nonlocal equations.

Conclusions

We have introduced a new approach to nonlocal advection, and, in particular, the nonlocal Burgers equation. This approach was inspired by the foundational approach to nonlocal mechanics developed in peridynamics. Analysis of the nonlocal advection equation we propose offers a logical path by which to address fundamental issues of shock phenomena—such as the formation of shock waves, entropy generation through shocks, properties of nonlocal viscous regularization—that must be addressed before a defensible shock physics implementation of peridynamics can be developed. We look forward to developing elements of this theory in future work.

Chapter 3

Peridynamics with LAMMPS: A User Guide

Introduction

This document details the implementation of a discrete peridynamic model within the LAMMPS molecular dynamic code, as described in the original article [46].

In §3 we discuss how to build the peridynamic module within LAMMPS, and discuss basic requirements for input scripts to use the peridynamic module. In §3 we overview the relevant portions of the peridynamic model of a continuum. In §3 we discuss the discretization of the peridynamic model and its LAMMPS implementation. Finally, in §3, we discuss a LAMMPS simulation of a specific numerical experiment described in [54].

Quick Start Guide

For those who hate reading users' guides[1], please try the following:

1. Download LAMMPS from `http://lammps.sandia.gov` and untar the source.
2. In the LAMMPS `src/` directory do `make yes-peri` followed by `make <your platform>` (for example, `make g++`).
3. In the LAMMPS `examples/peri` directory, run the example input script (for example, `lmp_g++ < in.peri`).
4. Follow instructions in §3 to visualize results.[2]

Typographical Conventions

Our typographical conventions are found in Table 3.1.

Finally, note all norms $\|\cdot\|$ are taken to be the 2-norm, $\|\cdot\|_2$.

[1] Congratulations on getting this far!

[2] For a more meaningful example, try running the input script in Algorithm 7 on page 37.

Getting Started

We assume that you already have a working LAMMPS installlation. For more on downloading and building LAMMPS, see `http://lammps.sandia.gov`. This document only provides information related to the peridynamic module within LAMMPS. For questions regarding the usage of LAMMPS, please see the LAMMPS documentation.

Building the Peridynamic Module within LAMMPS

In the LAMMPS distribution, the peridynamic model is distributed as an add-on module, which means that it is not by default compiled with the rest of LAMMPS. To instruct LAMMPS to build the peridynamic module, go to the LAMMPS source subdirectory (`/src`) and type

```
make yes-peri
```

followed by

```
make <your platform>
```

to compile LAMMPS on your particular platform.

Input Script Basics

Here we provide a listing of commands that must be included in a LAMMPS input script to utilize the peridynamic module. These commands assume knowledge of peridynamics (§3) and its discretization (§3). This is not an inclusive list of LAMMPS commands. For a complete example script, see §3.

LAMMPS has been modified to support SI units. To use SI units, your LAMMPS input script should contain the command

```
units si
```

Table 3.1. Notational conventions.

Notation	Example	Description
`Verbatim text`	`make g++`	Text to be typed at your command prompt
<text in angle brackets>	<your platform>	User specified statement
Bold lowercase letter	$\mathbf{x}$, $\boldsymbol{\xi}$	A vector in $\mathbb{R}^3$
Non-bold letter	K, α	A scalar in $\mathbb{R}$
Underlined lowercase letter	$\underline{t}$, $\underline{\omega}$	Scalar state (see §3)
Underlined bold uppercase letter	$\underline{\mathbf{T}}$, $\underline{\mathbf{M}}$	Vector state (see §3)

All quantities specified in the input script and data file, as well as quantities output to the screen, log file, and dump files will be in SI units.

Only a simple cubic lattice is currently supported. Your LAMMPS input script should contain the command

```
lattice sc <lattice constant>
```

A peridynamic simulation requires the "peri" atom style be used. Your input script should contain the command

```
atom_style peri
```

An associated required command tells LAMMPS to create a data structure used to index particles. Your input script should contain the command

```
atom_modify map array
```

The "skin" distance used when computing neighborlists should be defined appropriately for your choice of simulation parameters. Your input script should contain the command

```
neighbor <skin> bin
```

where the "skin" should be set to a value such that the peridynamic horizon plus the skin distance is larger than the maximum possible distance between two bonded particles (before their bond breaks). A peridynamic simulation also requires a peridynamic pair style be used. Your input script should contain either the commands

```
pair_style peri/lps
pair_coeff <type 1> <type 2> <bulk modulus> <shear modulus> <delta> <s00> <α>
```

to invoke the "peri/lps" pair style, or the commands

```
pair_style peri/pmb
pair_coeff <type 1> <type 2> <c> <delta> <s00> <α>
```

to invoke the "peri/pmb" pair style. See §3 for more on the linear peridynamic solid (LPS) model, and §3 for more on the prototype microelastic brittle (PMB) model.

The mass density and volume fraction for each particle must be defined. Your input script should contain the commands

```
set group all density <ρ>
set group all volume <Vi>
```

In the second line, you are setting the volume of each peridynamic particle. For a simple cubic lattice, the volume should be equal to the cube of the lattice constant, i.e., $V_i = \Delta x^3$.

If you wish to start a simulation with the velocity of the peridynamic particles set to zero, your input script should contain the command

```
velocity all set 0.0 0.0 0.0 sum no units box
```

We use a velocity-Verlet time integrator (algebraically equivalent to a centered difference in time, but numerically more stable.) To use a velocity-Verlet time integrator, your input script should contain the command

```
fix <fix id> all nve
```

You can compute the damage (see §3) at each particle with the compute style `damage/atom`:

```
compute <compute id> all damage/atom
```

To periodically dump snapshots of your simulation to disk, use the LAMMPS `dump` command:

```
dump <dump id> all custom <N> <dump filename> id type x y z c_<compute id>
```

where `N` is the number of steps between snapshots and `<compute id>` is the id of the `damage/atom` compute style above. You can visualize these snapshots (see §3).

Peridynamic Model of a Continuum

The following is not a complete overview of peridynamics, but a discussion of only those details specific to the model we have implemented within LAMMPS. For more on the peridynamic theory, the reader is referred to [55, 52]. To begin, we define the notation we will use.

Basic Notation

Within the peridynamic literature, the following notational conventions are generally used. The position of a given point in the reference configuration is $\mathbf{x}$. Let $\mathbf{u}(\mathbf{x}, t)$ and $\mathbf{y}(\mathbf{x}, t)$ denote the displacement and position, respectively, of the point $\mathbf{x}$ at time t. Define the relative position and displacement vectors of two bonded points $\mathbf{x}$ and $\mathbf{x}'$ as $\boldsymbol{\xi} = \mathbf{x}' - \mathbf{x}$ and $\boldsymbol{\eta} = \mathbf{u}(\mathbf{x}', t) - \mathbf{u}(\mathbf{x}, t)$, respectively. We note here that $\boldsymbol{\eta}$ is time-dependent, and that $\boldsymbol{\xi}$ is not. It follows that the relative position of the two bonded points in the current configuration can be written as $\boldsymbol{\xi} + \boldsymbol{\eta} = \mathbf{y}(\mathbf{x}', t) - \mathbf{y}(\mathbf{x}, t)$.

Peridynamic models are frequently written using *states*, which we briefly describe here. For the purposes of our discussion, all states are operators that act on vectors in $\mathbb{R}^3$. For a more complete

discussion of states, see [55]. A *vector state* is an operator whose image is a vector, and may be viewed as a generalization of a second-rank tensor. Similarly, a *scalar state* is an operator whose image is a scalar. Of particular interest is the vector force state $\underline{\mathbf{T}}\left[\mathbf{x},t\right]\left\langle \mathbf{x}'-\mathbf{x}\right\rangle$, which is a mapping, having units of force per volume squared, of the vector $\mathbf{x}'-\mathbf{x}$ to the force vector state field. The vector state operator $\underline{\mathbf{T}}$ may itself be a function of $\mathbf{x}$ and t. The constitutive model is completely contained within $\underline{\mathbf{T}}$.

In the peridynamic theory, the deformation at a point depends collectively on all points interacting with that point. Using the notation of [55], we write the peridynamic equation of motion as

$$\rho(\mathbf{x})\ddot{\mathbf{u}}(\mathbf{x},t)=\int_{\mathcal{H}_{\mathbf{x}}}\left\{\underline{\mathbf{T}}\left[\mathbf{x},t\right]\left\langle \mathbf{x}'-\mathbf{x}\right\rangle-\underline{\mathbf{T}}\left[\mathbf{x}',t\right]\left\langle \mathbf{x}-\mathbf{x}'\right\rangle\right\}dV_{\mathbf{x}'}+\mathbf{b}(\mathbf{x},t), \tag{3.0.1}$$

where ρ represents the mass density, $\underline{\mathbf{T}}$ the force vector state, and $\mathbf{b}$ an external body force density. A point $\mathbf{x}$ interacts with all the points $\mathbf{x}'$ within the neighborhood $\mathcal{H}_{\mathbf{x}}$, assumed to be a spherical region of radius $\delta>0$ centered at $\mathbf{x}$. δ is called the *horizon*, and is analogous to the cutoff radius used in molecular dynamics. Conditions on $\underline{\mathbf{T}}$ for which (3.0.1) satisfies the balance of linear and angular momentum are given in [55].

We consider only force vector states that can be written as

$$\underline{\mathbf{T}}=\underline{t}\,\underline{\mathbf{M}},$$

with $\underline{t}$ a *scalar force state* and $\underline{\mathbf{M}}$ the *deformed direction vector state*, defined by

$$\underline{\mathbf{M}}\left\langle \boldsymbol{\xi}\right\rangle=\begin{cases}\frac{\boldsymbol{\xi}+\boldsymbol{\eta}}{\|\boldsymbol{\xi}+\boldsymbol{\eta}\|} & \|\boldsymbol{\xi}+\boldsymbol{\eta}\|\neq 0\\ \mathbf{0} & \text{otherwise}\end{cases}. \tag{3.0.2}$$

Such force states correspond to so-called *ordinary* materials ([55]). These are the materials for which the force between any two interacting points $\mathbf{x}$ and $\mathbf{x}'$ acts along the line between the points.

Linear Peridynamic Solid (LPS) Model

We summarize the linear peridynamic solid (LPS) material model. For more on this model, the reader is referred to [55]. This model is a nonlocal analogue to a classical linear elastic isotropic material. The elastic properties of a a classical linear elastic isotropic material are determined by (for example) the bulk and shear moduli. For the LPS model, the elastic properties are analogously determined by the bulk and shear moduli, along with the horizon δ.

The LPS model has a force scalar state

$$\underline{t}=\frac{3K\theta}{m}\underline{\omega}\,\underline{x}+\alpha\underline{\omega}\,\underline{e}^{\mathrm{d}}, \tag{3.0.3}$$

with K the bulk modulus and α related to the shear modulus G as

$$\alpha=\frac{15G}{m}.$$

The remaining components of the model are described as follows. Define the reference position scalar state $\underline{x}$ so that $\underline{x}\left\langle \boldsymbol{\xi}\right\rangle=\|\boldsymbol{\xi}\|$. Then, the weighted volume m is defined as

$$m\left[\mathbf{x}\right]=\int_{\mathcal{H}_{\mathbf{x}}}\underline{\omega}\left\langle \boldsymbol{\xi}\right\rangle\underline{x}\left\langle \boldsymbol{\xi}\right\rangle\underline{x}\left\langle \boldsymbol{\xi}\right\rangle dV_{\boldsymbol{\xi}}. \tag{3.0.4}$$

Let

$$\underline{e}\left[\mathbf{x},t\right]\langle\boldsymbol{\xi}\rangle=\|\boldsymbol{\xi}+\boldsymbol{\eta}\|-\|\boldsymbol{\xi}\|$$

be the extension scalar state, and

$$\theta\left[\mathbf{x},t\right]=\frac{3}{m\left[\mathbf{x}\right]}\int_{\mathcal{H}_{\mathbf{x}}}\underline{\omega}\langle\boldsymbol{\xi}\rangle\,\underline{x}\langle\boldsymbol{\xi}\rangle\,\underline{e}\left[\mathbf{x},t\right]\langle\boldsymbol{\xi}\rangle\,dV_{\boldsymbol{\xi}}$$

be the dilatation. The isotropic and deviatoric parts of the extension scalar state are defined, respectively, as

$$\underline{e}^{\mathrm{i}}=\frac{\theta\underline{x}}{3},\qquad\underline{e}^{\mathrm{d}}=\underline{e}-\underline{e}^{\mathrm{i}},$$

where the arguments of the state functions and the vectors on which they operate are omitted for simplicity. We note that the LPS model is linear in the dilatation θ, and in the deviatoric part of the extension $\underline{e}^{\mathrm{d}}$.

Remark 3.0.1. The weighted volume m is time-independent, and does not change as bonds break. It is computed with respect to the bond family defined at the reference (initial) configuration.

The nonnegative scalar state $\underline{\omega}$ is an *influence function* [55, Defn. 3.2]. For more on influence functions, see [50]. If an influence function $\underline{\omega}$ depends only upon the scalar $\|\boldsymbol{\xi}\|$, (i.e., $\underline{\omega}\langle\boldsymbol{\xi}\rangle=\underline{\omega}\langle\|\boldsymbol{\xi}\|\rangle$), then $\underline{\omega}$ is a spherical influence function. For a spherical influence function, the LPS model is isotropic [55, Prop. 14.1].

Remark 3.0.2. In the PDLAMMPS implementation of the LPS model, the influence function $\underline{\omega}\langle\|\boldsymbol{\xi}\|\rangle=1/\|\boldsymbol{\xi}\|$ is used. However, the user can define their own influence function by altering the method `influence_function` in the file `pair_peri_lps.cpp`. The PDLAMMPS code permits both spherical and non-spherical influence functions (e.g., isotropic and non-isotropic materials).

Prototype Microelastic Brittle (PMB) Model

We summarize the prototype microelastic brittle (PMB) material model. For more on this model, the reader is referred to [52, 54]. This model is a special case of the LPS model; see [50] for the derivation. The elastic properties of the PMB model are determined by the bulk modulus K and the horizon δ.

The PMB model is expressed using the scalar force state field

$$\underline{t}\left[\mathbf{x},t\right]\langle\boldsymbol{\xi}\rangle=\frac{1}{2}f\left(\boldsymbol{\eta},\boldsymbol{\xi}\right),\tag{3.0.5}$$

with f a scalar-valued function. We assume that f takes the form

$$f=cs,$$

where

$$c=\frac{18K}{\pi\delta^4},\tag{3.0.6}$$

with K the bulk modulus and δ the horizon, and s the bond stretch, defined as

$$s(t,\boldsymbol{\eta},\boldsymbol{\xi})=\frac{\|\boldsymbol{\eta}+\boldsymbol{\xi}\|-\|\boldsymbol{\xi}\|}{\|\boldsymbol{\xi}\|}.$$

Bond stretch is a unitless quantity, and identical to a one-dimensional definition of strain. As such, we see that a bond at its equilibrium length has stretch $s = 0$, and a bond at twice its equilibrium length has stretch $s = 1$. The constant c given above is appropriate for 3D models only. For more on the origins of the constant c, see [54]. For the derivation of c for 1D and 2D models, see [17].

Given (3.0.5), (3.0.1) reduces to

$$\rho(\mathbf{x})\ddot{\mathbf{u}}(\mathbf{x},t) = \int_{\mathcal{H}_{\mathbf{x}}} \mathbf{f}\left(\boldsymbol{\eta},\boldsymbol{\xi}\right) dV_{\boldsymbol{\xi}} + \mathbf{b}(\mathbf{x},t), \tag{3.0.7}$$

with

$$\mathbf{f}\left(\boldsymbol{\eta},\boldsymbol{\xi}\right) = f\left(\boldsymbol{\eta},\boldsymbol{\xi}\right) \frac{\boldsymbol{\xi}+\boldsymbol{\eta}}{\|\boldsymbol{\xi}+\boldsymbol{\eta}\|}.$$

Unlike the LPS model, the PMB model has a Poisson ratio of $\nu = 1/4$ in 3D, and $\nu = 1/3$ in 2D. This is reflected in the input for the PMB model, which requires only the bulk modulus of the material, whereas the LPS model requires both the bulk and shear moduli.

Damage

Bonds are made to break when they are stretched beyond a given limit. Once a bond fails, it is failed forever [54]. Further, new bonds are never created during the course of a simulation. We discuss only one criterion for bond breaking, called the *critical stretch* criterion.

Define μ to be the history-dependent scalar boolean function

$$\mu(t,\boldsymbol{\eta},\boldsymbol{\xi}) = \left\{ \begin{array}{ll} 1 & \text{if } s(t',\boldsymbol{\eta},\boldsymbol{\xi}) < \min\left(s_0(t',\boldsymbol{\eta},\boldsymbol{\xi}), s_0(t',\boldsymbol{\eta}',\boldsymbol{\xi}')\right) \text{ for all } 0 \le t' \le t \\ 0 & \text{otherwise} \end{array} \right\}. \tag{3.0.8}$$

where $\boldsymbol{\eta}' = \mathbf{u}(\mathbf{x}'',t) - \mathbf{u}(\mathbf{x}',t)$ and $\boldsymbol{\xi}' = \mathbf{x}'' - \mathbf{x}'$. Here, $s_0(t,\boldsymbol{\eta},\boldsymbol{\xi})$ is a critical stretch defined as

$$s_0(t,\boldsymbol{\eta},\boldsymbol{\xi}) = s_{00} - \alpha s_{\min}(t,\boldsymbol{\eta},\boldsymbol{\xi}), \qquad s_{\min}(t) = \min_{\boldsymbol{\xi}} s(t,\boldsymbol{\eta},\boldsymbol{\xi}), \tag{3.0.9}$$

where s_{00} and α are material-dependant constants. The history function μ breaks bonds when the stretch s exceeds the critical stretch s_0.

Although $s_0(t,\boldsymbol{\eta},\boldsymbol{\xi})$ is expressed as a property of a particle, bond breaking must be a symmetric operation for all particle pairs sharing a bond. That is, particles $\mathbf{x}$ and $\mathbf{x}'$ must utilize the same test when deciding to break their common bond. This can be done by any method that treats the particles symmetrically. In the definition of μ above, we have chosen to take the minimum of the two s_0 values for particles $\mathbf{x}$ and $\mathbf{x}'$ when determining if the $\mathbf{x}$–$\mathbf{x}'$ bond should be broken.

Following [54], we can define the damage at a point $\mathbf{x}$ as

$$\varphi(\mathbf{x},t) = 1 - \frac{\int_{\mathcal{H}_{\mathbf{x}}} \mu(t,\boldsymbol{\eta},\boldsymbol{\xi}) dV_{\mathbf{x}'}}{\int_{\mathcal{H}_{\mathbf{x}}} dV_{\mathbf{x}'}}. \tag{3.0.10}$$

Discrete Peridynamic Model and LAMMPS Implementation

In LAMMPS, instead of (3.0.1), we model this equation of motion:

$$\rho(\mathbf{x})\ddot{\mathbf{y}}(\mathbf{x},t) = \int_{\mathcal{H}_{\mathbf{x}}} \left\{ \underline{\mathbf{T}}\left[\mathbf{x},t\right]\left\langle \mathbf{x}'-\mathbf{x}\right\rangle - \underline{\mathbf{T}}\left[\mathbf{x}',t\right]\left\langle \mathbf{x}-\mathbf{x}'\right\rangle \right\} dV_{\mathbf{x}'} + \mathbf{b}(\mathbf{x},t),$$

where we explicitly track and store at each timestep the positions and not the displacements of the particles. We observe that $\ddot{\mathbf{y}}(\mathbf{x},t) = \ddot{\mathbf{x}} + \ddot{\mathbf{u}}(\mathbf{x},t) = \ddot{\mathbf{u}}(\mathbf{x},t)$, so that this is equivalent to (3.0.1).

Spatial Discretization

The region defining a peridynamic material is discretized into particles forming a simple cubic lattice with lattice constant Δx, where each particle i is associated with some volume fraction V_i. For any particle i, let $\mathcal{F}_i$ denote the family of particles for which particle i shares a bond in the reference configuration. That is,

$$\mathcal{F}_i = \{p \mid \|\mathbf{x}_p - \mathbf{x}_i\| \leq \delta\}. \tag{3.0.11}$$

The discretized equation of motion replaces (3.0.1) with

$$\rho\ddot{\mathbf{y}}_i^n = \sum_{p\in\mathcal{F}_i} \left\{ \underline{\mathbf{T}}\left[\mathbf{x}_i,t\right]\left\langle \mathbf{x}_p'-\mathbf{x}_i\right\rangle - \underline{\mathbf{T}}\left[\mathbf{x}_p,t\right]\left\langle \mathbf{x}_i-\mathbf{x}_p\right\rangle \right\} V_p + \mathbf{b}_i^n, \tag{3.0.12}$$

where n is the timestep number and subscripts denote the particle number.

Short-Range Forces

In the model discussed so far, particles interact only through their bond forces. A particle with no bonds becomes a free non-interacting particle. To account for contact forces, short-range forces are introduced [53]. We add to the force in (3.0.12) the following force

$$\mathbf{f}_S(\mathbf{y}_p,\mathbf{y}_i) = \min\left\{0, \frac{c_S}{\delta}(\left\|\mathbf{y}_p-\mathbf{y}_i\right\| - d_{pi})\right\} \frac{\mathbf{y}_p-\mathbf{y}_i}{\left\|\mathbf{y}_p-\mathbf{y}_i\right\|}, \tag{3.0.13}$$

where d_{pi} is the short-range interaction distance between particles p and i, and c_S is a multiple of the constant c from (3.0.6). Note that the short-range force is always repulsive, never attractive. In practice, we choose

$$c_S = 15\frac{18K}{\pi\delta^4}. \tag{3.0.14}$$

For the short-range interaction distance, we choose [53]

$$d_{pi} = \min\left\{0.9\left\|\mathbf{x}_p-\mathbf{x}_i\right\|, 1.35(r_p+r_i)\right\}, \tag{3.0.15}$$

where r_i is called the *node radius* of particle i. Given a discrete lattice, we choose r_i to be half the lattice constant.[3] Given this definition of d_{pi}, contact forces appear only when particles are under compression.

[3]For a simple cubic lattice, $\Delta x = \Delta y = \Delta z$.

When accounting for short-range forces, it is convenient to define the short-range family of particles

$$\mathcal{F}_i^S = \{p \mid \left\|\mathbf{y}_p - \mathbf{y}_i\right\| \leq d_{pi}\}.$$

Modification to the Particle Volume

The right-hand side of (3.0.12) may be thought of as a midpoint quadrature of (3.0.1). To slightly improve the accuracy of this quadrature, we discuss a modification to the particle volume used in (3.0.12). In a situation where two particles share a bond with $\|\mathbf{x}_p - \mathbf{x}_i\| = \delta$, for example, we suppose that only approximately half the volume of each particle is "seen" by the other [53]. When computing the force of each particle on the other we use $V_p/2$ rather than V_p in (3.0.12). As such, we introduce a nodal volume scaling function for all bonded particles where $\delta - r_i \leq \|\mathbf{x}_p - \mathbf{x}_i\| \leq \delta$ (c.f. Figure 3.1).

We choose to use a linear unitless nodal volume scaling function

$$\nu(\mathbf{x}_p - \mathbf{x}_i) = \left\{ \begin{array}{cl} -\frac{1}{2r_i}\|\mathbf{x}_p - \mathbf{x}_i\| + \left(\frac{\delta}{2r_i} + \frac{1}{2}\right) & \text{if } \delta - r_i \leq \|\mathbf{x}_p - \mathbf{x}_i\| \leq \delta \\ 1 & \text{if } \|\mathbf{x}_p - \mathbf{x}_i\| \leq \delta - r_i \\ 0 & \text{otherwise} \end{array} \right\}$$

If $\|\mathbf{x}_p - \mathbf{x}_i\| = \delta$, $\nu = 0.5$, and if $\|\mathbf{x}_p - \mathbf{x}_i\| = \delta - r_i$, $\nu = 1.0$, for example.

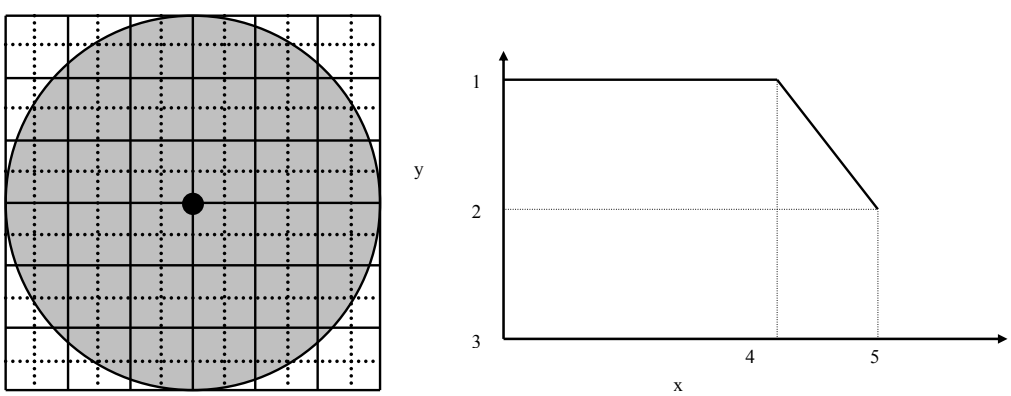

(a) Two-dimensional diagram showing particle on mesh (solid lines) with neighborhood $\mathcal{H}_\mathbf{x}$ as grey circular region. Dual mesh (dotted lines) shows boundaries of each particle.

(b) Plot of $\nu(\mathbf{x}_p - \mathbf{x}_i)$ vs. $\|\mathbf{x}_p - \mathbf{x}_i\|$.

Figure 3.1. Diagram showing horizon of a particular particle, demonstrating that the volume associated with particles near the boundary of the horizon is not completely contained within the horizon.

Temporal Discretization

When discretizing time in LAMMPS, we use a velocity-Verlet scheme, where both the position and velocity of the particle are stored explicitly. The velocity-Verlet scheme is generally expressed in three steps. In Algorithm 1, ρ_i denotes the mass density of a particle and $\widetilde{\mathbf{f}}_i^n$ denotes the the net force density on particle i at timestep n. The LAMMPS command `fix nve` performs a velocity-Verlet integration.

Algorithm 1 Velocity Verlet

1: $\mathbf{v}_i^{n+1/2} = \mathbf{v}_i^n + \frac{\Delta t}{2\rho_i}\widetilde{\mathbf{f}}_i^n$
2: $\mathbf{y}_i^{n+1} = \mathbf{y}_i^n + \Delta t \mathbf{v}_i^{n+1/2}$
3: $\mathbf{v}_i^{n+1} = \mathbf{v}_i^{n+1/2} + \frac{\Delta t}{2\rho_i}\widetilde{\mathbf{f}}_i^{n+1}$

Breaking Bonds

During the course of simulation, it may be necessary to break bonds, as described in §3. Bonds are recorded as broken in a simulation by removing them from the bond family $\mathcal{F}_i$ (see (3.0.11)).

A naïve implementation would have us first loop over all bonds and compute s_{min} in (3.0.9), then loop over all bonds again and break bonds with a stretch $s > s0$ as in (3.0.8), and finally loop over all particles and compute forces for the next step of Algorithm 1. For reasons of computational efficiency, we will utilize the values of s_0 from the *previous* timestep when deciding to break a bond.

Remark 3.0.3. For the first timestep, s_0 is initialized to ∞ for all nodes. This means that no bonds may be broken until the second timestep. As such, it is recommended that the first few timesteps of the peridynamic simulation not involve any actions that might result in the breaking of bonds. As a practical example, the projectile in §3 is placed such that it does not impact the target brittle plate until several timesteps into the simulation.

LPS Pseudocode

A sketch of the LPS model implementation in PDLAMMPS appears in Algorithm 2. This algorithm makes use of the routines in Algorithms 3 and 4.

PMB Pseudocode

A sketch of the PMB model implementation in PDLAMMPS appears in Algorithm 5.

Damage

The damage associated with every particle (see (3.0.10)) can optionally be computed and output with a LAMMPS data dump. To do this, your input script must contain the command

Algorithm 2 LPS Peridynamic Model Pseudocode

Fix s_{00}, α, horizon δ, bulk modulus K, shear modulus G, timestep Δt, and generate initial lattice of particles with lattice constant Δx. Let there be N particles. Define constant c_S for repulsive short-range forces.
Initialize bonds between all particles $i \neq j$ where $\|\mathbf{x}_j - \mathbf{x}_i\| \leq \delta$
Initialize weighted volume m for all particles using Algorithm 3
Initialize $s_0 = \infty$ {*Initialize each entry to MAX_DOUBLE*}
while not done **do**
  Perform step 1 of Algorithm 1, updating velocities of all particles
  Perform step 2 of Algorithm 1, updating positions of all particles
  $\tilde{s}_0 = \infty$ {*Initialize each entry to MAX_DOUBLE*}
  for $i = 1$ to N **do**
    {Compute short-range forces}
    for all particles $j \in \mathcal{F}_i^S$ (the short-range family of nodes for particle i) **do**
      $r = \left\|\mathbf{y}_j - \mathbf{y}_i\right\|$
      $dr = \min\{0, r - d\}$. {*Short-range forces are only repulsive, never attractive*}
      $k = \frac{c_S}{\delta} V_k dr$ {c_S *defined in* (3.0.14)}
      $\mathbf{f} = \mathbf{f} + k \frac{\mathbf{y}_j - \mathbf{y}_i}{\|\mathbf{y}_j - \mathbf{y}_i\|}$
    end for
  end for
  Compute the dilatation for each particle using Algorithm 4
  for $i = 1$ to N **do**
    {Compute bond forces}
    for all particles j sharing an unbroken bond with particle i **do**
      $e = \left\|\mathbf{y}_j - \mathbf{y}_i\right\| - \|\mathbf{x}_j - \mathbf{x}_i\|$
      $\omega_+ = \underline{\omega}\left\langle \mathbf{x}_j - \mathbf{x}_i \right\rangle$ {*Influence function evaluation*}
      $\omega_- = \underline{\omega}\left\langle \mathbf{x}_i - \mathbf{x}_j \right\rangle$ {*Influence function evaluation*}
      $\hat{f} = \left[(3K - 5G)\left(\frac{\theta(i)}{m(i)}\omega_+ + \frac{\theta(j)}{m(j)}\omega_-\right)\|\mathbf{x}_j - \mathbf{x}_i\| + 15G\left(\frac{\omega_+}{m(i)} + \frac{\omega_-}{m(j)}\right)e\right]\nu(\mathbf{x}_j - \mathbf{x}_i)V_j$
      $\mathbf{f} = \mathbf{f} + \hat{f}\frac{\mathbf{y}_j - \mathbf{y}_i}{\|\mathbf{y}_j - \mathbf{y}_i\|}$
      if $(dr/\|\mathbf{x}_j - \mathbf{x}_i\|) > \min(s_0(i), s_0(j))$ **then**
        Break i's bond with j {*j's bond with i will be broken when this loop iterates on j*}
      end if
      $\tilde{s}_0(i) = \min(\tilde{s}_0(i), s_{00} - \alpha(dr/\|\mathbf{x}_j - \mathbf{x}_i\|))$
    end for
  end for
  $s_0 = \tilde{s}_0$ {*Store for use in next timestep*}
  Perform step 3 of Algorithm 1, updating velocities of all particles
end while

Algorithm 3 Computation of Weighted Volume m

for $i = 1$ to N **do**
  $m(i) = 0.0$
  for all particles j sharing a bond with particle i **do**
    $m(i) = m(i) + \underline{\omega}\left\langle \mathbf{x}_j - \mathbf{x}_i \right\rangle \|\mathbf{x}_j - \mathbf{x}_i\|^2 \nu(\mathbf{x}_j - \mathbf{x}_i)V_j$
  end for
end for

Algorithm 4 Computation of Dilatation θ

for $i = 1$ to N **do**
  $\theta(i) = 0.0$
  for all particles j sharing an unbroken bond with particle i **do**
    $e = \left\|\mathbf{y}_i - \mathbf{y}_j\right\| - \|\mathbf{x}_i - \mathbf{x}_j\|$
    $\theta(i) = \theta(i) + \underline{\omega}\left\langle \mathbf{x}_j - \mathbf{x}_i \right\rangle \|\mathbf{x}_j - \mathbf{x}_i\| e\nu(\mathbf{x}_j - \mathbf{x}_i)V_j$
  end for
  $\theta(i) = \frac{3}{m(i)}\theta(i)$
end for

Algorithm 5 PMB Peridynamic Model Pseudocode

```
Fix s_00, α, horizon δ, spring constant c, timestep Δt, and generate initial lattice of particles with lattice constant
  Δx. Let there be N particles.
Initialize bonds between all particles i ≠ j where ‖x_j − x_i‖ ≤ δ
Initialize s_0 = ∞ {Initialize each entry to MAX_DOUBLE}
while not done do
    Perform step 1 of Algorithm 1, updating velocities of all particles
    Perform step 2 of Algorithm 1, updating positions of all particles
    s̃_0 = ∞ {Initialize each entry to MAX_DOUBLE}
    for i = 1 to N do
        {Compute short-range forces}
        for all particles j ∈ F_i^S (the short-range family of nodes for particle i) do
            r = ‖y_j − y_i‖
            dr = min{0, r − d} {Short-range forces are only repulsive, never attractive}
            k = (c_S/δ) V_k dr {c_S defined in (3.0.14)}
            f = f + k (y_j − y_i)/‖y_j − y_i‖
        end for
    end for
    for i = 1 to N do
        {Compute bond forces}
        for all particles j sharing an unbroken bond with particle i do
            r = ‖y_j − y_i‖
            dr = r − ‖x_j − x_i‖
            k = (c/‖x_i − x_j‖) ν(x_i − x_j) V_j dr {c defined in (3.0.6)}
            f = f + k (y_j − y_i)/‖y_j − y_i‖
            if (dr/‖x_j − x_i‖) > min(s_0(i), s_0(j)) then
                Break i's bond with j {j's bond with i will be broken when this loop iterates on j}
            end if
            s̃_0(i) = min(s̃_0(i), s_00 − α(dr/‖x_j − x_i‖))
        end for
    end for
    s_0 = s̃_0 {Store for use in next timestep}
    Perform step 3 of Algorithm 1, updating velocities of all particles
end while
```

Algorithm 6 Example Python Script to Convert LAMMPS Dump to Ensight .case File Format

```
import sys
from dump import dump
from ensight import ensight
d = dump("dump.peri");
d.map(1,"id",2,"type",3,"x",4,"y",5,"z",6,"damage");
e = ensight(d);
e.one("disk","damage","Damage")
```

```
compute <ComputeID> all damage/atom
```

This enables a LAMMPS per-atom compute to calculate the damage associated with each particle every time a LAMMPS data dump is called. To output the results of this compute in your dump file, you must use the LAMMPS `dump` command, as

```
dump <DumpID> all custom <N> <output filename> id type x y z c_<ComputeID>
```

where `N` is the number of timesteps between dumps.

Visualizing Simulation Results

LAMMPS does not visualize your simulation results. You'll need to post-process your LAMMPS data dump for use by a third-party visualization tool. Use of the pizza.py toolkit [47] is recommended for conversion of LAMMPS data dump to another format suitable for use of your visualization package of choice.

As an example, we outline here one possible means of visualizing the output of a peridynamic simulation using only freely available open-source software. We assume that you have a dump file named `dump.peri` constructed using line 35 in Algorithm 7, and that you have Algorithm 6 saved as a python script named `convert.py`.

1. Install the pizza.py toolkit from `http://www.sandia.gov/~sjplimp/pizza.html`.
2. Install the `Numeric` Python packages from `http://sourceforge.net/projects/numpy/files/Old%20Numeric/`. The package is installed correctly if you can type `>>> import Numeric` from an interactive python prompt.
3. Install ParaView from `www.paraview.org`.
4. Run the conversion script: `python convert.py`.

This will produce an Ensight-format `.case` file, as well as a `.xyz` file and a `.damage` file. Launch ParaView, open the `.case` file, and click the green `Apply` button on the left. For more on Paraview, see `www.paraview.org`.

Pitfalls

Parallel Scalability. LAMMPS operates in parallel in a spatial-decomposition mode [48], where each processor owns a spatial subdomain of the overall simulation domain and communicates with its neighboring processors via distributed-memory message passing (MPI) [58] to acquire ghost atom information to allow forces on the atoms it owns to be computed. LAMMPS also uses Verlet neighbor lists which are recomputed every few timesteps as particles move. On these timesteps, particles also migrate to new processors as needed. LAMMPS decomposes the overall simulation domain so that spatial subdomains of nearly equal volume are assigned to each processor. When each subdomain contains nearly the same number of particles, this results in a reasonable load balance among all processors. As is more typical with some peridynamic simulations, some subdomains may contain many particles while other subdomains contain few particles, resulting in a load imbalance that impacts parallel scalability.

Setting the "skin" distance. The `neighbor` command with LAMMPS is used to set the so-called "skin" distance used when building neighbor lists. All atom pairs within a cutoff distance equal to the horizon δ plus the skin distance are stored in the list. Unexpected crashes in LAMMPS may be due to too small a skin distance. The skin should be set to a value such that δ plus the skin distance is larger than the maximum possible distance between two bonded particles. For example, if s_{00} is increased, the skin distance may also need to be increased.

"Lost" particles. All particles are contained within the "simulation box" of LAMMPS. The boundaries of this box may change with time, or not, depending on how the LAMMPS `boundary` command has been set. If a particle drifts outside the simulation box during the course of a simulation, it is called *lost*.

As an option of the `themo_modify` command of LAMMPS, the lost keyword determines whether LAMMPS checks for lost atoms each time it computes thermodynamics and what it does if atoms are lost. If the value is `ignore`, LAMMPS does not check for lost atoms. If the value is `error` or `warn`, LAMMPS checks and either issues an error or warning. The code will exit with an error and continue with a warning. This can be a useful debugging option. The default behavior of LAMMPS is to exit with an error if a particle is lost.

The peridynamic module within LAMMPS does not check for lost atoms. If a particle with unbroken bonds is lost, those bonds are marked as broken by the remaining particles.

Defining the peridynamic horizon δ. In the `pair_coeff` command, the user must specify the horizon δ. This argument determines which particles are bonded when the simulation is initialized. It is recommended that δ be set to a small fraction of a lattice constant larger than desired.

For example, if the lattice constant is 0.0005 and you wish to set the horizon to three times the lattice constant, then set δ to be 0.0015001, a value slightly larger than three times the lattice constant. This guarantees that particles three lattice constants away from each other are still bonded. If δ is set to 0.0015, for example, floating point error may result in some pairs of particles three lattice constants apart not being bonded.

Breaking bonds too early. For technical reasons, the bonds in the simulation are not created until the end of the first timestep of the simulation. Therefore, one should not attempt to break bonds until at least the second step of the simulation.

Bugs

The user is cautioned that this code is a beta release. If you are confident that you have found a bug in the peridynamic module, please send an email to the developers. First, check the "New features and bug fixes" section of the LAMMPS website site to see if the bug has already been reported or fixed. If not, the most useful thing you can do for us is to isolate the problem. Run it on the smallest number of atoms and fewest number of processors and with the simplest input script that reproduces the bug. In your email, describe the problem and any ideas you have as to what is causing it or where in the code the problem might be. We'll request your input script and data files if necessary.

Modifying and Extending the Peridynamic Module

To add new features or peridynamic potentials to the peridynamic module, the user is referred to section 8 of the LAMMPS user manual, *Modifying & extending LAMMPS*. To develop a new bond-based material, start with the PMB pair style as a template. To develop a new state-based material, start with the LPS pair style as a template.

A Numerical Example

To introduce the peridynamic implementation within LAMMPS, we replicate a numerical experiment taken from section 6 of [54].

Problem Description and Setup

We consider the impact of a rigid sphere on a homogeneous disk of brittle material. The sphere has diameter 0.01 m and velocity 100 m/s directed normal to the surface of the target. The target material has density $\rho = 2200$ kg/m^3. A PMB material model is used with $K = 14.9$ GPa and critical bond stretch parameters given by $s_{00} = 0.0005$ and $\alpha = 0.25$. A three-dimensional simple cubic lattice is constructed with lattice constant 0.0005 m and horizon 0.0015 m. (The horizon is three times the lattice constant.) The target is a cylinder of diameter 0.074 m and thickness 0.0025 m, and the associated lattice contains 103,110 particles. Each particle i has volume fraction $V_i = 1.25 \times 10^{-10}$ m^3.

The spring constant in the PMB material model is (see (3.0.6))

$$c = \frac{18k}{\pi\delta^4} = \frac{18(14.9 \times 10^9)}{\pi(1.5 \times 10^{-3})^4} \approx 1.6863 \times 10^{22}.$$

The CFL analysis from [54] shows that a timestep of 1.0×10^{-7} is safe.

We observe here that in IEEE double-precision floating point arithmetic when computing the bond stretch $s(t, \boldsymbol{\eta}, \boldsymbol{\xi})$ at each iteration where $\|\boldsymbol{\eta} + \boldsymbol{\xi}\|$ is computed during the iteration and $\|\boldsymbol{\xi}\|$ was computed and stored for the initial lattice, it may be that $fl(s) = \varepsilon$ with $|\varepsilon| \leq \varepsilon_{machine}$ for an unstretched bond. Taking $\varepsilon = 2.220446049250313 \times 10^{-16}$, we see that the value $csV_i \approx 4.68 \times 10^{-4}$, computed when determining f, is perhaps larger than we would like, especially when the true force should be zero. One simple way to avoid this issue is to insert the following instructions in Algorithm 5 after instruction 21 (and similarly for Algorithm 2):

1: **if** $|dr| < \varepsilon_{machine}$ **then**
2: $\quad dr = 0.$
3: **end if**

Qualitatively, this says that displacements from equilibrium on the order of 10^{-6}Å are taken to be exactly zero, a seemingly reasonable assumption.

The Projectile

The projectile used in the following experiments is not the one used in [54]. The projectile used here exerts a force

$$F(r) = -k_s(r - R)^2$$

on each atom where k_s is a specified force constant, r is the distance from the atom to the center of the indenter, and R is the radius of the projectile. The force is repulsive and $F(r) = 0$ for $r > R$. For our problem, the projectile radius $R = 0.05$ m, and we have chosen $k_s = 1.0 \times 10^{17}$ (compare with (3.0.6) above).

Writing the LAMMPS Input File

We discuss the example input script from Algorithm 7. In line 2 we specify that SI units are to be used. We specify the dimension (3) and boundary conditions ("shrink-wrapped") for the computational domain in lines 3 and 4. In line 5 we specify that peridynamic particles are to be used for this simulation. In line 7, we set the "skin" distance used in building the LAMMPS neighborlist. In line 8 we set the lattice constant (in meters) and in line 10 we define the spatial region where the target will be placed. In line 12 we specify a rectangular box enclosing the target region that defines the simulation domain. Line 14 fills the target region with atoms. Lines 15 and 17 define the peridynamic material model, and lines 19 and 21 set the particle density and particle volume, respectively. The particle volume should be set to the cube of the lattice constant for a simple cubic lattice. Line 23 sets the initial velocity of all particles to zero. Line 25 instructs LAMMPS to integrate time with velocity-Verlet, and lines 27-30 create the spherical projectile, sending it with a velocity of 100 m/s towards the target. Line 32 declares a compute style for the damage (percentage of broken bonds) associated with each particle. Line 33 sets the timestep, line 34 instructs LAMMPS to provide a screen dump of thermodynamic quantities every 200 timesteps, and line 35 instructs LAMMPS to create a data file (`dump.peri`) with a complete snapshot of the system every 100 timesteps. This file can be used to create still images or movies. Finally, line 36 instructs LAMMPS to run for 2,000 timesteps.

Algorithm 7 Example LAMMPS Input Script

```
1: # 3D Peridynamic simulation with projectile
2: units           si
3: dimension       3
4: boundary        s s s
5: atom_style      peri
6: atom_modify     map array
7: neighbor        0.0010 bin
8: lattice         sc 0.0005
9: # Create desired target
10: region         target cylinder y 0.0 0.0 0.037 -0.0025 0.0 units box
11: # Make 1 atom type
12: create_box     1 target
13: # Create the atoms in the simulation region
14: create_atoms   1 region target
15: pair_style     peri/pmb [4]
16: #              <type1> <type2>    <c>    <horizon>  <s00> <alpha>
17: pair_coeff        *       *    1.6863e22 0.0015001 0.0005  0.25
18: # Set mass density
19: set            group all density 2200
20: # volume = lattice constant^3
21: set            group all volume 1.25e-10
22: # Zero out velocities of particles
23: velocity       all set 0.0 0.0 0.0 sum no units box
24: # Use velocity-Verlet time integrator
25: fix            F1 all nve
26: # Construct spherical indenter to shatter target
27: variable       y0 equal 0.00510
28: variable       vy equal -100
29: variable       y equal "v_y0 + step*dt*v_vy"
30: fix            F2 all indent 1e17 sphere 0.0000 v_y 0.0000 0.0050 units box
31: # Compute damage for each particle
32: compute        C1 all damage/atom
33: timestep       1.0e-7
34: thermo         200
35: dump           D1 all custom 100 dump.peri id type x y z c_C1
36: run            2000
```

Numerical Results and Discussion

We ran the input script from Algorithm 7. Images of the disk (projectile not shown) appear in Figure 3.2. The LAMMPS dump file was converted to an EnSight data format with the pizza.py toolkit [47]. Visualization was done with the EnSight visualization package [10]. Use of the Paraview visualization package is also recommended, as it reads EnSight data files, and is open-source and freely available [29]. See §3 for more on visualizing peridynamic simulations results. The plot of damage on the top monolayer was created by coloring each particle according to its damage (see (3.0.10)).

The symmetry in the computed solution arises because a "perfect" lattice was used, and a because a perfectly spherical projectile impacted the lattice at its geometric center. To break the symmetry in the solution, the nodes in the peridynamic body may be perturbed slightly from the lattice sites. To do this, a perturbed lattice of points can be prepared in a data file and read into

[4] To use the LPS model, replace line 15 with `pair_style peri/lps` and modify line 17 accordingly; see page 23.

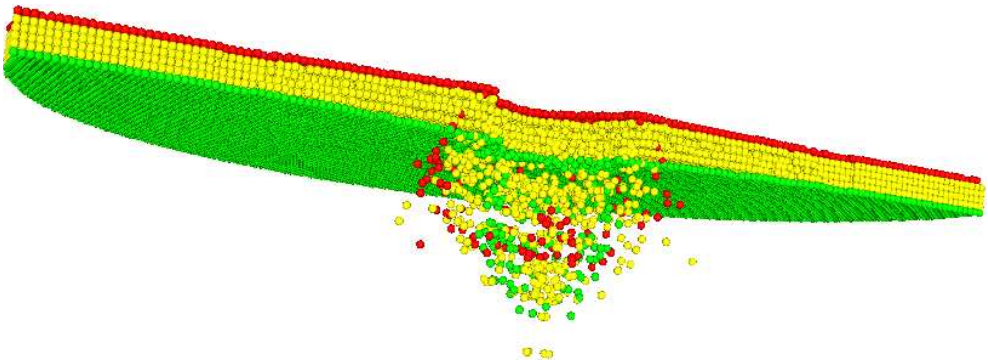

(a) Cut view of target during impact.

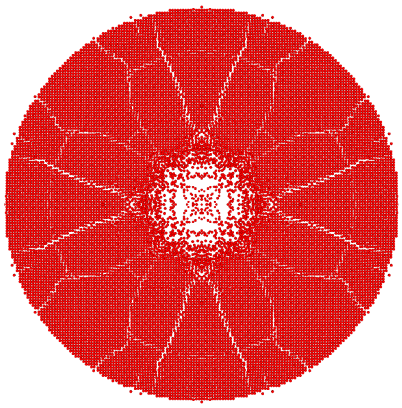

(b) Top monolayer showing fragmentation.

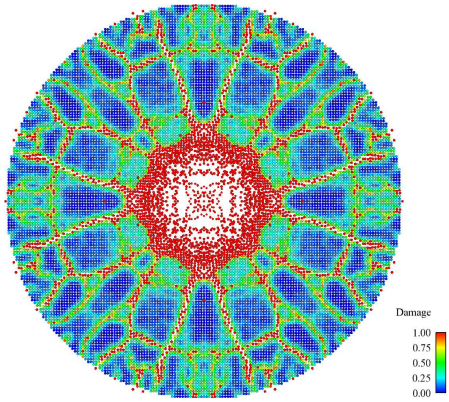

(c) Top monolayer showing damage. (blue = 0% broken bonds; red = 100% broken bonds)

Figure 3.2. Target during (a) and after (b,c) impact.

LAMMPS using the `read_data` command.

Chapter 4

The mapping from particle mechanics to continuum mechanics

This paper discusses the exact mapping from classical particle mechanics to the dynamical equations of continuum mechanics. The original work of Irving and Kirkwood and later that of Hardy is extended to systems with general multibody interactions. The approach of this paper can be used to derive continuum equations for a single instance (e.g. from molecular dynamics) or for an ensemble of systems, and in either case these systems can be very far from equilibrium. The interpretation of the continuum field quantities is that they represent observed densities which are spatial averages of microscopic densities. We derive a simple theorem about the consequences of reflection invariance with the important result that the Cauchy stress is symmetric if and only if the underlying potential is reflection invariant. The relation of the dynamical stress to virial stress is explored. For the energy equation some partitioning of the potential energy is required and we find that there is an additional microscopic heat source, which we call churning heat. We show that this vanishes for pair potentials and in the virial limit for three particle interactions; we conjecture that it always vanishes in the virial limit.

Introduction.

There are several different definitions of stress available in the literature. We distinguish conceptually between stress as a physical field that can be measured (in principle) and stress as the output of some model (e.g. an elastic or other particular phenomenological model): the latter is not of interest in this paper. The physical definitions can be divided generally into mechanical definitions (stress is the response to a virtual strain), thermodynamic definitions (stress is an average quantity derived from a virial theorem), and dynamical definitions (stress is that field which causes the momentum balance equation to be satisfied).

The approach taken in this paper is a dynamical one, since we show that this approach allows the construction of microscopic definitions of continuum fields which obey expected continuum balance laws. These definitions are valid even when the underlying system is very far from equilibrium, in great contrast to the mechanical and virial/thermodynamic definitions. This also means that we can show that the continuum balance laws are consequences of an underlying theory that is based on particles. This gives us a methodology for reasoning about the continuum balance laws which is not possible in a purely mathematical approach where these balance laws are taken to be postulates. Note also that we do not assume any results from the continuum theory but instead stop at developing the microscopic definitions of some of the quantities which appear in that theory.

The first serious attempt at constructing the dynamical stress was carried out in the seminal paper of Irving and Kirkwood [26]. Here a statistical ensemble of systems obeying classical particle mechanics was assumed and the continuum equations were derived using Liouville's theorem. This paper did not derive a closed form expression for the microscopic dynamical stress. Instead the potential part of the stress was shown to be the expectation of an infinite sum of distributions

$$\boldsymbol{\sigma}_{\mathrm{U}}^{\mu\nu}(\mathbf{x}) = \frac{1}{2}\left\langle \sum_{jk} \frac{\partial U_{jk}}{\partial \mathbf{x}_j^{\mu}} (\mathbf{x}_j - \mathbf{x}_k)^{\nu} \left\{ 1 - \frac{1}{2!}\mathbf{x}_{jk}\cdot\nabla_{\mathbf{x}} + \cdots + \frac{(-1)^n}{n!}\left(\mathbf{x}_{jk}\cdot\nabla_{\mathbf{x}}\right)^{n-1} + \cdots \right\} \delta(\mathbf{x}_j - \mathbf{x}) \right\rangle . \quad (4.0.1)$$

Noll [45, 33] was able to replace the sum of distributions with a pair of integrals

$$\boldsymbol{\sigma}_{\mathrm{U}}^{\mu\nu} = \frac{1}{2}\sum_{jk}\int_{\mathbf{z}} \frac{\mathbf{z}^{\mu}\mathbf{z}^{\nu}}{|\mathbf{z}|} \left.\frac{dU_{jk}(y)}{dy}\right|_{|\mathbf{z}|} \times \int_0^1 d\alpha \, \langle W | \mathbf{x}_j = \mathbf{x} + \alpha\mathbf{z}, \mathbf{x}_k = \mathbf{x} - (1-\alpha)\mathbf{z}) \rangle , \quad (4.0.2)$$

but neither of these formulas is useful from a computational point of view, and any connection with mechanical or virial definitions of stress is obviously very obscure. This approach was therefore more or less abandoned in the physical chemistry community. In developing what is now known as the Green-Kubo formalism Green [20] thus took a line of reasoning based on the virial theorem and the assumption of systems at equilibrium. Such techniques do not result in a stress that is part of a dynamical system of equations; instead they compute linear transport coefficients directly.

The next major advance in the computation of dynamical stress was due to Hardy [23]. This approach was developed explicitly for shock waves where the concept of equilibrium at the shock front is obviously problematic, so the equilibrium/virial methods are not applicable. Hardy introduced the concept of observed density fields which are spatial averages of microscopic densities. If the averaging filter (Hardy's localization function) is sufficiently sharp one can recover the microscopic densities, so mathematically nothing is lost. Hardy's formula for the potential part of the stress in terms of the pair force $\mathbf{f}_{jk}$ is

$$\boldsymbol{\sigma}_{\mathrm{U}}^{\mu\nu} = \frac{1}{2}\sum_{jk} \mathbf{f}_{jk}^{\nu}\mathbf{x}_{jk}^{\mu}\beta_{jk} \quad (4.0.3)$$

where β is the bond function derived from the averaging filter. This is clearly very close to the well known virial formula [62, 41]

$$\boldsymbol{\sigma}_{\mathrm{U}}^{\mu\nu} = \frac{1}{2V}\sum_{jk} \mathbf{f}_{jk}^{\nu}\mathbf{x}_{jk}^{\mu} \quad (4.0.4)$$

where V is the averaging volume. In this paper we show that (4.0.3) is equal to (4.0.4) in the limit of a very soft averaging function. Thus the Hardy and virial results are very closely related.

A second major advance due to Irving and Kirkwood [26] is the derivation of a continuum energy equation and the realization by these authors that the expression for heat flux follows from the derivation of stress by closing the energy balance equation. Of course this derivation suffers from the same problems that the original stress derivation has, but this difficulty was solved also by Hardy [23].

Thus we have a complete set of microscopic expressions for all the dynamical quantities that appear in the continuum equations, at least for pair potentials. We note that all of the references cited so far had carried out calculations only in this case, that is when the potential energy of all the particles is given as a sum of pairwise terms (equivalently, central forces) which depend only on the distance between the individual pair of particles. This is a valuable case to study, since it includes so-called simple fluids [22, 5]. But modern molecular dynamics calculations abound with multibody terms involving bond angles and torsion angles, not to mention terms such as the Axelrod-Teller [3, 43] interaction or Stillinger-Weber [59] type potentials. Although there have been attempts at generalizing microscopic stress formulas to more general potentials these have typically been carried out in a very ad-hoc fashion.

The main goal of this paper is to construct exact (and computable) expressions for microscopic stress and heat flux which are valid for any multibody potential. In order to carry out this goal we find that it is necessary to understand the concept of pair force in some detail. We find that a simplification is available if we add one additional symmetry principle, that of reflection invariance, to the underlying system. We are able to show that this constraint implies a simple formula for the pair force and as an important consequence we are able to show that symmetry of the Cauchy stress follows from reflection invariance of the underlying potential. This is in strong contrast to the understanding in the continuum mechanics community [40] that symmetry of the Cauchy stress is related to conservation of angular momentum.

For the energy equation it is also necessary to pick some partitioning for the potential energy, that is some assignment of parts of the potential energy to the individual particles. The arbitrariness in this procedure has been understood for a long time [26, 20], even for pair potentials. We carry out the analysis for an arbitrary partitioning and show that non-pair terms in the potential lead to a new kind of term in the heat flux. For multibody potentials we suggest the somewhat obvious idea of evenly dividing a given multibody term among the particles that participate in it. For three-body terms we are able to show that this partitioning leads to a churning term which vanishes in the virial limit and we conjecture that this is true for terms with more particles as well.

The outline of this paper is as follows. First we discuss the equations of continuum mechanics and the continuum field quantities. Then we introduce the particle mechanics model and derive the basic formula for pair forces that will be needed, including the theorems about the consequences of reflection invariance. The definition of microscopic and observed density fields is presented and the next sections show the derivation for the mass, momentum, and energy equations along with a discussion of the relation between the Hardy approach and the ensemble approach.

Continuum mechanics.

The goal of this paper is to derive the dynamical equations of continuum mechanics from a microscopic particle theory. Continuum mechanics is described by fields which represent mass density, material velocity, stress, energy density, heat flux. We expect to derive the conservation laws (balance equations) for mass, momentum, and energy which describe the connection between these field quantities. We use Eulerian form to avoid the necessity of introducing extraneous concepts (material points, bodies, deformation, and so forth). The end result will be a microscopic description of all the field quantities in the balance equations; this allows us to derive continuum mechanics from microscopic principles rather than postulating it as a mathematical theory.

Mass density.

The usual form for the balance equation describing conservation of mass is

$$\frac{\partial \rho}{\partial t} + \frac{\partial}{\partial \mathbf{x}^\mu}(\rho \mathbf{v}^\mu) = 0 \tag{4.0.5}$$

where ρ is the mass density and $\mathbf{v}$ is the material velocity. Alternatively, we can write

$$\frac{\partial \rho}{\partial t} + \frac{\partial}{\partial \mathbf{x}^\mu}(\boldsymbol{\pi}^\mu) = 0 \tag{4.0.6}$$

where $\boldsymbol{\pi} = \rho \mathbf{v}$ is the momentum density of the material. We use the Einstein summation convention for coordinate indices.

Momentum density.

The conservation equation for momentum is

$$\frac{\partial}{\partial t}(\rho \mathbf{v}^\nu) + \frac{\partial}{\partial \mathbf{x}^\mu}(\rho \mathbf{v}^\mu \mathbf{v}^\nu) = \frac{\partial \boldsymbol{\sigma}^{\mu\nu}}{\partial \mathbf{x}^\mu} \tag{4.0.7}$$

or

$$\frac{\partial}{\partial t}(\boldsymbol{\pi}^\nu) + \frac{\partial}{\partial \mathbf{x}^\mu}(\mathbf{v}^\mu \boldsymbol{\pi}^\nu) = \frac{\partial \boldsymbol{\sigma}^{\mu\nu}}{\partial \mathbf{x}^\mu} \tag{4.0.8}$$

where we introduce the tensor Cauchy stress field $\boldsymbol{\sigma}$.

Total and internal energy densities.

There are two equations describing conservation of energy. Let ϵ be the total material energy density. Then

$$\frac{\partial \epsilon}{\partial t} + \frac{\partial}{\partial \mathbf{x}^\mu}(\epsilon \mathbf{v}^\mu) = \frac{\partial}{\partial \mathbf{x}^\mu}(\mathbf{v}^\nu \boldsymbol{\sigma}^{\mu\nu} - \mathbf{q}^\mu) \tag{4.0.9}$$

where $\mathbf{q}$ is the heat flux.

An additional equation is obtained by contracting (4.0.8) with $\mathbf{v}^\nu$ and subtracting from the energy conservation equation (4.0.9). The result is an equation for internal energy density, defined as the total energy density minus the material kinetic energy density. Thus,

$$\frac{\partial \epsilon_{\mathrm{I}}}{\partial t} + \frac{\partial}{\partial \mathbf{x}^\mu}(\epsilon_{\mathrm{I}} \mathbf{v}^\mu) = \frac{\partial \mathbf{v}^\nu}{\partial \mathbf{x}^\mu} \boldsymbol{\sigma}^{\mu\nu} - \frac{\partial \mathbf{q}^\mu}{\partial \mathbf{x}^\mu} \tag{4.0.10}$$

where

$$\epsilon_{\mathrm{I}} = \epsilon - \frac{1}{2}\rho \mathbf{v}^2 \tag{4.0.11}$$

Note that this equation contains terms which are all invariant under Galilean transformation, i.e. the equation is the same in a uniformly moving coordinate system.

Particle mechanics.

Hamiltonian particle mechanics.

Consider a system with N classical point particles with masses m_j, positions $\mathbf{x}_j(t)$, velocities $\mathbf{v}_j(t)$, and momenta $\mathbf{p}_j = m_j\mathbf{v}_j$. The particles follow Hamiltonian dynamics [31, 30] under the influence of a Hamiltonian H given by

$$H = K + U \tag{4.0.12}$$

where the kinetic energy K is the sum of the individual particle kinetic energies

$$K = \sum_j \frac{\mathbf{p}_j^2}{2m_j} \tag{4.0.13}$$

and the potential energy U is a given function of all the particle coordinates:

$$U = U(\mathbf{x}_1, \mathbf{x}_2, \cdots). \tag{4.0.14}$$

Often the assumption is made that U is a sum of pair contributions. We will avoid this assumption in most circumstances.

Note that we do not consider external forces; this is a fairly trivial modification to make.

We assume that U is independent of space and time, and invariant under rotations and translations. (Later we will see that U must be invariant under reflections as well). The usual equations of motion follow:

$$\begin{aligned} \frac{d\mathbf{x}_j}{dt} &= \frac{\mathbf{p}_j}{m_j} = \mathbf{v}_j \\ \frac{d\mathbf{p}_j}{dt} &= -\frac{\partial U}{\partial \mathbf{x}_j} \end{aligned} \tag{4.0.15}$$

Note that this dynamics can just as easily be derived from a Lagrangian formulation [31].

Conservation laws.

From the particle theory we can easily deduce the usual conservation laws for total mass, momentum, and energy. According to Noether's theorem [30] these conservation laws follow from the continuous symmetry principles that we assume for the Hamiltonian. The conservation of total mass M is trivial

$$M = \sum_j m_j \text{ and } \frac{dM}{dt} = 0. \tag{4.0.16}$$

The conservation of total momentum $\mathbf{P}$ is deduced from translational invariance and we have

$$\mathbf{P} = \sum_j \mathbf{p}_j \text{ and } \frac{d\mathbf{P}}{dt} = 0. \tag{4.0.17}$$

From rotational invariance we derive the conservation of total angular momentum $\mathbf{L}$

$$\mathbf{L} = \sum_j m_j \mathbf{x}_j \times \mathbf{v}_j \text{ and } \frac{d\mathbf{L}}{dt} = 0. \tag{4.0.18}$$

Note that this conservation law does not depend on the assumption of reflection invariance.

Finally, the conservation of total energy E follows from the independence of the Hamiltonian on time:

$$E = H \text{ and } \frac{dE}{dt} = 0. \tag{4.0.19}$$

Galilean invariance.

A Galilean transformation is a transformation to a new coordinate system $t', \mathbf{x}'$ where $t' = t$ and $\mathbf{x}' = \mathbf{x} + t\mathbf{V}$ for some constant velocity $\mathbf{V}$. Differences in coordinates are invariant under such a transformation, while velocities $\mathbf{v}$ are transformed to $\mathbf{v} + \mathbf{V}$. Thus velocity differences (and velocity gradients) are also invariant. Note that

$$\frac{\partial f}{\partial t} \to \frac{\partial f}{\partial t'} + \frac{\partial f}{\partial \mathbf{x}'^{\mu}} \mathbf{V}^{\mu} \tag{4.0.20}$$

while

$$\frac{\partial f}{\partial \mathbf{x}'^{\mu}} \to \frac{\partial f}{\partial \mathbf{x}^{\mu}}. \tag{4.0.21}$$

Decomposition of the force.

The force on particle j is defined as

$$\mathbf{F}_j = -\frac{\partial U}{\partial \mathbf{x}_j} \tag{4.0.22}$$

and from translational invariance we have

$$\sum_j \mathbf{F}_j = 0. \tag{4.0.23}$$

It is usual to introduce pair forces at this point. The pair force $\mathbf{f}_{jk}$ is intuitively defined as "the force on particle j due to particle k", with

$$\mathbf{F}_j = \sum_k \mathbf{f}_{jk} \tag{4.0.24}$$

(we will implicitly take $\mathbf{f}_{jj} = 0$ to simplify the notation in what follows). For the simplest case where U is given by a sum of pair contributions the pair force is easily computed.

The problem for a general potential U is that we have to decide how to decompose the forces into pair contributions. The above equation is not sufficient to determine this decomposition for large numbers of particles, because there are N particles but $O(N^2)$ possible pair force contributions.

Even if we add the constraint that $\mathbf{f}_{jk} = -\mathbf{f}_{kj}$ we still cannot uniquely determine the pair forces. This can be easily seen for as few as three particles, since we can write a transformed set of $\mathbf{f}_{jk}$:

$$\mathbf{f}'_{12} = \mathbf{f}_{12} + \mathbf{a}, \mathbf{f}'_{13} = \mathbf{f}_{13}, -\mathbf{a}, \text{ and } \mathbf{f}'_{23} = \mathbf{f}_{23} + \mathbf{a} \tag{4.0.25}$$

that leaves $\mathbf{F}_j$ invariant for an arbitrary vector $\mathbf{a}$. Note that a restriction that $\mathbf{a}$ must be some function of the particle coordinates is insufficient, since we could take $\mathbf{a} = K(\mathbf{x}_1 - \mathbf{x}_2)$ for some arbitrary K. Thus particle forces $\mathbf{F}_j$ are well defined but they do not determine a unique pairwise decomposition, and therefore pairwise forces are not measurable physical quantities. A definition is necessary and the results will depend on that definition.

A possible definition of the pair force is given by the following argument [41]. Since U is translationally invariant, it can only depend on the differences between particle positions. So we can define

$$\mathbf{f}_{jk} = -\frac{1}{2}\frac{\partial U}{\partial \mathbf{x}_{jk}} \tag{4.0.26}$$

where $\mathbf{x}_{jk} = \mathbf{x}_j - \mathbf{x}_k$. Note that this definition satisfies the requirement (Newton's third law) that

$$\mathbf{f}_{jk} = -\mathbf{f}_{kj}. \tag{4.0.27}$$

and of course we can easily show that these pair forces satisfy (4.0.24). We will see that this definition has problems, but first we examine this in the context of Newton's third law.

(4.0.27) shows that pair forces are equal and opposite, but not necessarily directed along the line between two particles. This can be seen by looking at forces generated by a potential among four particles $\mathbf{x}_0, \mathbf{x}_1, \mathbf{x}_2, \mathbf{x}_3$ of the form

$$U = (\mathbf{x}_1 - \mathbf{x}_0) \cdot ((\mathbf{x}_2 - \mathbf{x}_0) \times (\mathbf{x}_3 - \mathbf{x}_0)). \tag{4.0.28}$$

Such a term is invariant under translations and rotations, but not reflections, and the resulting forces do not obey the strong form of Newton's third law. Using (4.0.26) we get

$$\begin{aligned}
\mathbf{f}_{01} &= -(\mathbf{x}_2 - \mathbf{x}_0) \times (\mathbf{x}_3 - \mathbf{x}_0) \\
\mathbf{f}_{02} &= (\mathbf{x}_1 - \mathbf{x}_0) \times (\mathbf{x}_3 - \mathbf{x}_0) \\
\mathbf{f}_{03} &= -(\mathbf{x}_1 - \mathbf{x}_0) \times (\mathbf{x}_2 - \mathbf{x}_0) \\
\mathbf{f}_{12} &= 0 \\
\mathbf{f}_{13} &= 0 \\
\mathbf{f}_{23} &= 0.
\end{aligned} \tag{4.0.29}$$

so $\mathbf{f}_{01}$ is not parallel to $\mathbf{x}_0 - \mathbf{x}_1$, etc.

We can prove that the pair forces for this example cannot be written so that all of them lie along the direction of the pairs, even if we use the freedom described in (4.0.25) to modify them. To see this, choose the triangles $1, 2, 3$ for a vector $\mathbf{a}$, $1, 2, 4$ for a vector $\mathbf{b}$, and triangle $1, 3, 4$ for a vector $\mathbf{c}$. Then

$$\begin{aligned}
\mathbf{f}_{01} &\to \mathbf{f}_{01} + \mathbf{a} + \mathbf{b} \\
\mathbf{f}_{02} &\to \mathbf{f}_{02} - \mathbf{a} + \mathbf{c} \\
\mathbf{f}_{03} &\to \mathbf{f}_{03} - \mathbf{b} - \mathbf{c} \\
\mathbf{f}_{12} &\to \mathbf{f}_{12} + \mathbf{a} \\
\mathbf{f}_{13} &\to \mathbf{f}_{13} + \mathbf{b} \\
\mathbf{f}_{23} &\to \mathbf{f}_{23} + \mathbf{c}
\end{aligned} \tag{4.0.30}$$

where we attempt to choose $\mathbf{a}, \mathbf{b}, \mathbf{c}$ to enforce the strong law. This is as much freedom as is available; if we choose $\mathbf{d}$ from the triangle $2, 3, 4$ then it can be absorbed into a redefinition of $\mathbf{a}, \mathbf{b}, \mathbf{c}$. From the last three equations we see that to get $\mathbf{f}_{12}$ etc to lie in the direction $\mathbf{x}_{12}$ we must choose

$$\begin{aligned} \mathbf{a} &= K_{12}\mathbf{x}_{12} \\ \mathbf{b} &= K_{13}\mathbf{x}_{13} \\ \mathbf{c} &= K_{23}\mathbf{x}_{23} \end{aligned} \tag{4.0.31}$$

where K_{23}, K_{24}, K_{34} are scalars. Now consider the modified version of $\mathbf{f}_{01}$ which we want to lie in the direction $\mathbf{x}_{01}$. This becomes

$$\mathbf{f}_{01} = -\mathbf{x}_{02} \times \mathbf{x}_{03} + K_{12}\mathbf{x}_{12} + K_{13}\mathbf{x}_{13} = K_{01}\mathbf{x}_{01} \tag{4.0.32}$$

and using $\mathbf{x}_{12} = \mathbf{x}_{02} - \mathbf{x}_{01}$ etc. we can write

$$-\mathbf{x}_{02} \times \mathbf{x}_{03} + K_{12}\mathbf{x}_{02} - K_{12}\mathbf{x}_{01} + K_{13}\mathbf{x}_{03} - K_{13}\mathbf{x}_{01} = K_{01}\mathbf{x}_{01}. \tag{4.0.33}$$

But now if $\mathbf{x}_{01}$ and $\mathbf{x}_{02}$ are chosen in one plane and we assume that $\mathbf{x}_{03}$ is perpendicular to that plane we see that on the left hand side there is a vector proportional to $\mathbf{x}_{03}$ while on the right hand side there is none. Therefore the equation cannot be satisfied and there is generally no way to rewrite the forces so they satify the strong form of Newton's third law.

If we add reflection invariance to the symmetries of the potential U then we can deduce a form for the pair force that is both equal and opposite and directed along the line between the pair. Indeed, we can show that U is a function of pair distances $d_{jk} = |\mathbf{x}_{jk}|$ if and only if it is invariant under reflections as well as translations and rotations.

When U has the given symmetries we can construct the positions of the particles from the distances between particles (pair distances) modulo a symmetry group operation as follows: Assume that the first four particles are not in a degenerate configuration and that all the pair distances are given (we actually only need the distances to the first four particles). Begin by translating and rotating such that the first particle is at the origin, the second particle lies on the positive x axis, and the third lies in the upper half of the x, y plane. The fourth particle can be placed in a tetrahedral position either above or below this plane. By reflection we can choose arbitrarily either one side or the other. Now for all the remaining particles we have more distances than are needed to locate them with respect to the first four. For each additional particle we can use the distances to the first three particles to find two possible locations above and below the x, y plane but because of the additional constraint of the distance to the fourth particle there will be only one solution that is feasible. Therefore there is a unique (modulo a symmetry group operation) mapping from distances to the particle positions.

Practical molecular dynamics simulations often use potentials written in terms of pairwise distances, bond angles, and bond torsions; in the appendix we derive some simple formulas for conversion of these angle terms to functions of pairwise distances.

Given U as a function of pair distances we can use the chain rule to write the total force on particle j as

$$\mathbf{F}_j = -\frac{1}{2}\sum_{kl} \frac{\partial d_{kl}}{\partial \mathbf{x}_j}\frac{\partial U}{\partial d_{kl}}, \tag{4.0.34}$$

where we make the notation simpler by ignoring the $k = l$ term and summing over all possible k and l. The factor of $1/2$ takes care of the double counting of terms. Of course

$$\frac{\partial d_{kl}}{\partial \mathbf{x}_j} = \mathbf{x}_{kl}\frac{1}{d_{kl}}(\delta_{jk} - \delta_{jl}) \tag{4.0.35}$$

so that

$$\mathbf{F}_j = -\sum_k (\mathbf{x}_j - \mathbf{x}_k)\frac{1}{d_{jk}}\frac{\partial U}{\partial d_{jk}}. \tag{4.0.36}$$

We can now define the pair force

$$\mathbf{f}_{jk} = -(\mathbf{x}_j - \mathbf{x}_k)\frac{1}{d_{jk}}\frac{\partial U}{\partial d_{jk}}. \tag{4.0.37}$$

where $\mathbf{f}_{jk}$ satisfies (4.0.24) and the strong form of Newton's third law by construction.

An alternative expression uses distance parameters ξ_{jk} defined by

$$\xi_{jk} = \frac{1}{2}d_{jk}^2 \tag{4.0.38}$$

so that

$$\mathbf{f}_{jk} = -(\mathbf{x}_j - \mathbf{x}_k)G_{jk} \tag{4.0.39}$$

where the generalized force G_{jk} is defined by

$$G_{jk} = \frac{\partial U}{\partial \xi_{jk}} = \frac{1}{d_{jk}}\frac{\partial U}{\partial d_{jk}}. \tag{4.0.40}$$

The advantage of this form over (4.0.37) is that we get rid of the factor of $1/d_{jk}$ with its attendant singularity.

The equations (4.0.39) and (4.0.37) do not give the same results as (4.0.26), even when the potential is reflection invariant. Consider a simple three particle term which is a dot product

$$U = (\mathbf{x}_1 - \mathbf{x}_3)\cdot(\mathbf{x}_2 - \mathbf{x}_3). \tag{4.0.41}$$

Using (4.0.26) we obtain the following pair forces

$$\begin{aligned} \mathbf{f}_{12} &= 0 \\ \mathbf{f}_{13} &= -(\mathbf{x}_2 - \mathbf{x}_3) \\ \mathbf{f}_{23} &= -(\mathbf{x}_1 - \mathbf{x}_3) \end{aligned} \tag{4.0.42}$$

but we can also write (see (4.0.145) in the appendix)

$$\begin{aligned} U &= \xi_{13} + \xi_{23} - \xi_{12} \\ &= \frac{1}{2}((\mathbf{x}_1 - \mathbf{x}_3)^2 + (\mathbf{x}_2 - \mathbf{x}_3)^2 - (\mathbf{x}_1 - \mathbf{x}_2)^2) \\ &= (\mathbf{x}_1 - \mathbf{x}_3)\cdot(\mathbf{x}_2 - \mathbf{x}_3). \end{aligned} \tag{4.0.43}$$

and we obtain from (4.0.39) the pair forces

$$\begin{aligned} \mathbf{f}_{12} &= \mathbf{x}_1 - \mathbf{x}_2 \\ \mathbf{f}_{13} &= -(\mathbf{x}_1 - \mathbf{x}_3) \\ \mathbf{f}_{23} &= -(\mathbf{x}_2 - \mathbf{x}_3) \end{aligned} \tag{4.0.44}$$

which are clearly not the same as (4.0.26).

These sets must be physically equivalent, since they both give the same total force on each particle. Indeed, we can use $\mathbf{a} = \mathbf{x}_1 - \mathbf{x}_2$ in the transformation (4.0.25) to map (4.0.42) onto (4.0.39). This example thus serves to illustrate the difficulty in defining precisely the term "pair force". In the remainder of the paper we will generally assume the existence of reflection invariance for the potential and will use the definition (4.0.39).

Note that when G_{jk} is positive the force is attractive since the force on particle j points from particle j to particle k and vice versa. Also, clearly we have $G_{jk} = G_{kj}$.

If U is given as a sum of pair potentials U_{jk} then it is useful to have a formula for the pair force in terms of the pair potential. We begin with

$$U = \frac{1}{2}\sum_{jk} U_{jk} \tag{4.0.45}$$

where we sum over all particles j, k and divide by two because of the double counting. We can assume that $U_{jj} = 0$ to simplify the notation. Then

$$\begin{aligned} G_{jk} &= \frac{\partial U}{\partial \xi_{jk}} = \frac{1}{2}(U'_{jk} + U'_{kj}) \\ &= U'_{jk} \end{aligned} \tag{4.0.46}$$

where U'_{jk} is the derivative of U_{jk} wrt ξ_{jk}. Therefore in this case

$$\mathbf{f}_{jk} = -(\mathbf{x}_j - \mathbf{x}_k)U'_{jk}. \tag{4.0.47}$$

Further discussion about reflection invariance.

Another way to look at the consequence of reflection invariance is as follows. Suppose U is invariant under reflection R, then it must be true from (4.0.26) that under R

$$\mathbf{f}_{jk} \underset{R}{\rightarrow} -\mathbf{f}_{jk} \tag{4.0.48}$$

Now consider

$$\mathbf{f}_{jk} \times (\mathbf{x}_j - \mathbf{x}_k) \underset{R}{\rightarrow} \mathbf{f}_{ij} \times (\mathbf{x}_j - \mathbf{x}_k) \tag{4.0.49}$$

so this vector is invariant under reflection. We now argue that this must be zero, because any such vector must be translation invariant and constructible from the relative particle positions $\mathbf{x}_{jk}$ which all invert under reflection. Multiplying one of these expressions by a pseudoscalar will not work because we can then show that U would not be reflection invariant.

Conversely, if U is not reflection invariant then we can divide it into two parts one of which is invariant and the other which is a pseudoscalar. The pseudoscalar term will lead to a component such that

$$\mathbf{f}_{jk} \times (\mathbf{x}_j - \mathbf{x}_k) \neq 0. \tag{4.0.50}$$

We thus see that the strong form of Newton's third law is true if and only if U is invariant under translations, rotations and reflections. If U is invariant only under translations and rotations but not reflections then we have only the weak form of the third law.

Microscopic densities.

The definitions of microscopic densities for mass and momentum are straightforward. We simply associate a delta function with each particle that follows the particle around. The delta function for mass density is weighted by the mass of that particle while the delta function for momentum density is weighted by the momentum of the particle. Thus the microscopic mass density $\hat{\rho}$ is

$$\hat{\rho}(\mathbf{x}, t) = \sum_j m_j \delta(\mathbf{x} - \mathbf{x}_j) \tag{4.0.51}$$

while that for microscopic momentum density is

$$\hat{\boldsymbol{\pi}}(\mathbf{x}, t) = \sum_j m_j \mathbf{v}_j \delta(\mathbf{x} - \mathbf{x}_j). \tag{4.0.52}$$

On the other hand the microscopic energy density is not so straightforward to define. The kinetic part of the energy due to each particle can be assigned to the particle, but the potential energy must be distributed among the particles. Thus we take

$$U = \sum_j U^{(j)} \tag{4.0.53}$$

where $U^{(j)}$ represents the part of the potential energy assigned to particle j. This partitioning is still somewhat arbitrary at this point, but we will assume that the partitions depend only on the particle positions and that they satisfy the same symmetries that U does. The microscopic energy density is thus given by

$$\hat{\epsilon}(\mathbf{x}, t) = \sum_j \left(\frac{1}{2} m_j \mathbf{v}_j^2 + U^{(j)} \right) \delta(\mathbf{x} - \mathbf{x}_j) \tag{4.0.54}$$

From the above definitions we can easily see that the total mass, total momentum, and total energy are conserved, because

$$\int \hat{\rho} = M, \int \hat{\boldsymbol{\pi}} = \mathbf{P}, \text{ and } \int \hat{\epsilon} = E. \tag{4.0.55}$$

Observed densities.

We assume that the densities that an observer would see are given by spatial averages of the microscopic densities. The spatial average is defined by some experimental filter function ϕ, so that the observed mass density is given by

$$\rho(\mathbf{x}, t) = \int \phi(\mathbf{x}, \mathbf{x}') \hat{\rho}(\mathbf{x}', t) d\mathbf{x}' \tag{4.0.56}$$

The filter function must have some simple properties in order to make the observed densities physically meaningful. In particular ϕ must be independent of space and time, we must have $\phi \geq 0$, and

$$\int \phi = 1. \tag{4.0.57}$$

Finally, we take ϕ to be rotationally invariant (if not then the observed densities will not be rotationally invariant). From these properties we deduce that ϕ depends only on $|\mathbf{x}-\mathbf{x}'|$.

The observed mass density is thus given by the expression

$$\rho(\mathbf{x},t) = \sum_j m_j \phi(\mathbf{x}-\mathbf{x}_j) \tag{4.0.58}$$

where the spatial dependence arises from the appearance of $\mathbf{x}$ and the time dependence comes from the dependence on $\mathbf{x}_j(t)$. We introduce the notation

$$\phi_j = \phi(\mathbf{x}-\mathbf{x}_j). \tag{4.0.59}$$

and the above equation can be written

$$\rho(\mathbf{x},t) = \sum_j m_j \phi_j \tag{4.0.60}$$

We can easily derive the simple relation

$$\frac{\partial \phi_j}{\partial t} = -\mathbf{v}_j^\mu \frac{\partial \phi_j}{\partial \mathbf{x}^\mu} \tag{4.0.61}$$

that will be used repeatedly in the following.

The observed momentum density is easily seen to be

$$\boldsymbol{\pi}(\mathbf{x},t) = \sum_j m_j \mathbf{v}_j \phi_j \tag{4.0.62}$$

and the observed energy density is

$$\epsilon(\mathbf{x},t) = \sum_j \left(\frac{1}{2} m_j \mathbf{v}_j^2 + U^{(j)}\right) \phi_j \tag{4.0.63}$$

Note that from (4.0.57) we see that the observed densities also represent conserved quantities. In particular

$$\int \rho = M, \int \boldsymbol{\pi} = \mathbf{P}, \text{ and } \int \epsilon = E. \tag{4.0.64}$$

independent of time.

Conservation of mass.

Consider the observed mass density ρ. Using the definition (4.0.60) and the relation (4.0.61) we get

$$\begin{aligned} \frac{\partial \rho}{\partial t} &= -\sum_j m_j \mathbf{v}_j^\mu \frac{\partial \phi_j}{\partial \mathbf{x}^\mu} \\ &= -\frac{\partial}{\partial \mathbf{x}^\mu}\left(\sum_j m_j \mathbf{v}_j^\mu \phi_j\right) \\ &= -\frac{\partial}{\partial \mathbf{x}^\mu} \boldsymbol{\pi}^\mu \end{aligned} \tag{4.0.65}$$

where the second line follows from the fact that neither m_j nor $\mathbf{v}_j$ depend on the spatial coordinate $\mathbf{x}$.

We can deduce the continuum equation for conservation of mass (4.0.5) if the material velocity field $\mathbf{v}$ is *defined* with the relation

$$\boldsymbol{\pi} = \rho \mathbf{v} \tag{4.0.66}$$

so that the microscopic definition of material velocity is the mass-weighted quantity

$$\mathbf{v} = \frac{\sum_j m_j \mathbf{v}_j \phi_j}{\sum_j m_j \phi_j}. \tag{4.0.67}$$

Note that although material velocity does have a microscopic definition it is not a density. One could possibly make a different definition of material velocity but it might be very difficult to show that mass, momentum, and energy were conserved.

At this point we can define relative particle velocities $\mathbf{u}_j$ with

$$\mathbf{v}_j = \mathbf{v} + \mathbf{u}_j \tag{4.0.68}$$

and we note that the definition of the material velocity implies the relation

$$\sum_j m_j \mathbf{u}_j = 0 \tag{4.0.69}$$

The absolute particle velocities are independent of $\mathbf{x}$ but it is important to realise that the relative particle velocities have a dependence on $\mathbf{x}$ through their dependence on the material velocity. Therefore in some of the following derivations we must be very careful to commute the gradient operator with absolute particle velocities, not relative ones.

We can now show that the definition of "material point" is problematic, and therefore the usual transformation to material coordinates may not be possible. We attempt to construct the material coordinate at spatial position $\mathbf{x}$ as the localized center of mass coordinate, similar to the localized mass-weighted velocity that we identified as material velocity. This gives

$$\mathbf{y} = \frac{\sum_j m_j \mathbf{x}_j \phi_j}{\sum_j m_j \phi_j}. \tag{4.0.70}$$

and we can define the relative particle position $\mathbf{d}_j$ as

$$\mathbf{d}_j = \mathbf{x}_j - \mathbf{y}. \tag{4.0.71}$$

Note that $\dot{\mathbf{d}}_j \neq \mathbf{u}_j$. Now we can show that

$$\frac{\partial \mathbf{y}}{\partial t} + \frac{\partial}{\partial \mathbf{x}^\mu}(\mathbf{v}^\mu \mathbf{y}) = \mathbf{v} + \frac{\partial}{\partial \mathbf{x}^\mu}\left(\sum_j m_j \mathbf{u}_j \mathbf{d}_j \phi_j\right). \tag{4.0.72}$$

so that $\mathbf{y}$ is not a material coordinate since the quantity in parentheses does not vanish. An alternative approach is to define the material coordinate as an interpolation of the particle coordinates in some way. If this is done then the material velocity is still not the time derivative of the material

coordinate (or, if it is forced to be then mass is not conserved). Yet another alternative approach is to define the material coordinate by back integration in time of the material velocity; here the difficulty is to prove that the resulting coordinate is some reasonably simple function of the particle positions and that the coordinate is single valued.

Thus, the usual transformation to material coordinates that is typically made in continuum mechanics is not necessarily possible. For this reason, any use of material coordinates has been omitted from this paper.

Conservation of momentum.

We straightforwardly differentiate (4.0.62) with respect to time to get

$$\frac{\partial \boldsymbol{\pi}^\nu}{\partial t} = \sum_j m_j \mathbf{v}_j^\nu \frac{\partial \phi_j}{\partial t} + \sum_j m_j \frac{\partial \mathbf{v}_j^\nu}{\partial t} \phi_j \tag{4.0.73}$$

We use the same process as for the conservation of mass to rewrite the first term and we use the equation of motion (4.0.15) for the second term. Thus

$$\frac{\partial \boldsymbol{\pi}^\nu}{\partial t} = -\frac{\partial}{\partial \mathbf{x}^\mu} \left(\sum_j m_j \mathbf{v}_j^\mu \mathbf{v}_j^\nu \phi_j \right) - \sum_j \frac{\partial U}{\partial \mathbf{x}_j^\nu} \phi_j. \tag{4.0.74}$$

Now substitute the relative velocities (4.0.68) in the expression

$$\begin{aligned} \sum_j m_j \mathbf{v}_j^\mu \mathbf{v}_j^\nu \phi_j = \mathbf{v}^\mu \mathbf{v}^\nu \sum_j m_j \phi_j \\ + \mathbf{v}^\mu \sum_j m_j \mathbf{u}_j^\nu \phi_j \\ + \mathbf{v}^\nu \sum_j m_j \mathbf{u}_j^\mu \phi_j \\ + \sum_j m_j \mathbf{u}_j^\mu \mathbf{u}_j^\nu \phi_j \end{aligned} \tag{4.0.75}$$

and the two inner sums vanish from (4.0.69) so we have

$$\sum_j m_j \mathbf{v}_j^\mu \mathbf{v}_j^\nu \phi_j = \rho \mathbf{v}^\mu \mathbf{v}^\nu + \sum_j m_j \mathbf{u}_j^\mu \mathbf{u}_j^\nu \phi_j. \tag{4.0.76}$$

This leads to

$$\frac{\partial \boldsymbol{\pi}^\nu}{\partial t} + \frac{\partial (\rho \mathbf{v}^\mu \mathbf{v}^\nu)}{\partial \mathbf{x}^\mu} = \frac{\partial}{\partial \mathbf{x}^\mu} \boldsymbol{\sigma}_{\mathrm{K}}^{\mu\nu} - \sum_j \frac{\partial U}{\partial \mathbf{x}_j^\nu} \phi_j \tag{4.0.77}$$

where we define the kinetic part of the stress as

$$\boldsymbol{\sigma}_{\mathrm{K}}^{\mu\nu} = -\sum_j m_j \mathbf{u}_j^\mu \mathbf{u}_j^\nu \phi_j. \tag{4.0.78}$$

We now treat the second sum. Using the force decomposition (4.0.26) we have

$$\begin{aligned} -\sum_j \frac{\partial U}{\partial \mathbf{x}_j^\nu}\phi_j &= \sum_{jk} \mathbf{f}_{jk}^\nu \phi_j \\ &= \frac{1}{2}\sum_{jk} \mathbf{f}_{jk}^\nu (\phi_j - \phi_k) \end{aligned} \tag{4.0.79}$$

using the fact that $\mathbf{f}_{jk}$ is antisymmetric under interchange of the indices.

Under the assumption of reflection invariance we can use (4.0.39) to see that

$$-\sum_j \frac{\partial U}{\partial \mathbf{x}_j^\nu}\phi_j = -\frac{1}{2}\sum_{jk} (\mathbf{x}_j^\nu - \mathbf{x}_k^\nu) G_{jk}(\phi_j - \phi_k) \tag{4.0.80}$$

Evidently to build an expression for microscopic stress we must be able to turn $\phi_j - \phi_k$ into the divergence of some quantity. There are several ways to accomplish this; we will skip the less useful approaches of Irving-Kirkwood [26] and Noll [44] and focus on that of Hardy [23] and the Fourier aspect of the method developed originally by Green [20]. We will see that these methods are closely related to each other and to the result of the virial method.

Hardy's method.

Hardy [23] introduced a *bond function* β_{jk} defined by

$$\beta_{jk} = \int_0^1 \phi(\mathbf{x} - \lambda \mathbf{x}_j - (1-\lambda)\mathbf{x}_k)\, d\lambda \tag{4.0.81}$$

which has the property that

$$\phi_j - \phi_k = -\frac{\partial}{\partial \mathbf{x}^\mu}(\mathbf{x}_{jk}^\mu \beta_{jk}). \tag{4.0.82}$$

This allows us to write

$$\frac{\partial \boldsymbol{\pi}^\nu}{\partial t} + \frac{\partial \rho \mathbf{v}^\mu \mathbf{v}^\nu}{\partial \mathbf{x}^\mu} = \frac{\partial}{\partial \mathbf{x}^\mu}\boldsymbol{\sigma}_{\mathrm{K}}^{\mu\nu} + \frac{\partial}{\partial \mathbf{x}^\mu}\boldsymbol{\sigma}_{\mathrm{U}}^{\mu\nu} \tag{4.0.83}$$

where

$$\boldsymbol{\sigma}_{\mathrm{U}}^{\mu\nu} = -\frac{1}{2}\sum_{jk} \mathbf{f}_{jk}^\nu \mathbf{x}_{jk}^\mu \beta_{jk} \tag{4.0.84}$$

So far we have written the microscopic stress in terms of a pair force $\mathbf{f}_{jk}$ without making the assumption of reflection invariance. If the potential is not reflection invariant then the pair force will not be proportional to $\mathbf{x}_{jk}$ and the Cauchy stress is not symmetric. On the other hand if we do assume reflection invariance then we can use (4.0.39) to write

$$\boldsymbol{\sigma}_{\mathrm{U}}^{\mu\nu} = \frac{1}{2}\sum_{jk} G_{jk}\mathbf{x}_{jk}^\nu \mathbf{x}_{jk}^\mu \beta_{jk} \tag{4.0.85}$$

which is explicitly symmetric. Therefore we have established the result that the Cauchy stress is symmetric if and only if the underlying potential is reflection invariant.

From (4.0.57) and (4.0.81) we see that

$$\int \beta_{jk} = 1 \tag{4.0.86}$$

and we also note that β_{kj} has units of 1/volume. For a very soft filter function ϕ we can replace ϕ and β with $1/V$ where V is an averaging volume. The precise meaning of this is better described with the Fourier approach.

A simpler form is available when U consists of pair terms. Using (4.0.46) we obtain

$$\boldsymbol{\sigma}_{\mathrm{U}}^{\mu\nu} = \frac{1}{2}\sum_{jk} U'_{jk}\mathbf{x}_{jk}^{\nu}\mathbf{x}_{jk}^{\mu}\beta_{jk} \tag{4.0.87}$$

The Fourier method.

A version of the Fourier method was introduced by Green [20]. See also Hansen and McDonald [22], and references therein.

Consider the Fourier transform of the function $\phi_j - \phi_k$. This is

$$\begin{aligned}\hat{\phi}_j(\mathbf{k}) - \hat{\phi}_k(\mathbf{k}) &= \hat{\phi}(\mathbf{k})\left(e^{i\mathbf{k}\cdot\mathbf{x}_j} - e^{i\mathbf{k}\cdot\mathbf{x}_k}\right) \\ &= i\mathbf{k}\cdot\mathbf{x}_{jk}\hat{\phi}(\mathbf{k})\frac{e^{i\mathbf{k}\cdot\mathbf{x}_j} - e^{i\mathbf{k}\cdot\mathbf{x}_k}}{i\mathbf{k}\cdot\mathbf{x}_{jk}}\end{aligned} \tag{4.0.88}$$

Using the usual properties of Fourier transform we can derive

$$\boldsymbol{\sigma}_{\mathrm{U}}^{\mu\nu} = \frac{1}{2}\sum_{jk} \mathbf{f}_{jk}^{\nu}\mathbf{x}_{jk}^{\mu}\beta_{jk} \tag{4.0.89}$$

where the Fourier transform of β_{jk} is given by

$$\hat{\beta}_{jk}(\mathbf{k}) = \hat{\phi}(\mathbf{k})\frac{e^{i\mathbf{k}\cdot\mathbf{x}_j} - e^{i\mathbf{k}\cdot\mathbf{x}_k}}{i\mathbf{k}\cdot\mathbf{x}_{jk}} \tag{4.0.90}$$

and we can easily show that this is equal to the Fourier transform of Hardy's bond function.

Conservation of angular momentum.

The usual derivation [40] of a balance equation which describes continuum conservation of angular momentum relies on two assumptions. The first assumption is that the material angular momentum density can be written as

$$\mathbf{l} = \rho\mathbf{y}\times\mathbf{v} \tag{4.0.91}$$

where $\mathbf{y}$ is the material coordinate which obeys the equation

$$\frac{\partial\mathbf{y}}{\partial t} = \mathbf{v}. \tag{4.0.92}$$

The second assumption is that the Cauchy stress is symmetric. From this one can show that

$$\frac{\partial \mathbf{l}}{\partial t} + \frac{\partial}{\partial \mathbf{x}^\mu}\mathbf{v}^\mu \mathbf{l} = 0. \tag{4.0.93}$$

The conclusion from this argument is that angular momentum is conserved if and only if the Cauchy stress is symmetric.

We have seen above that symmetry of the Cauchy stress is not a consequence of conservation of angular momentum but instead relies on the assumption of microscopic reflection invariance. Therefore we need to resolve the difference between these arguments.

The point of view taken in this paper is that the angular momentum density $\mathbf{l}$ defined above does not represent a meaningful angular momentum density, because $\mathbf{y}$ is not necessarily a meaningful physical quantity. Therefore the classical continuum mechanics argument is unphysical and not relevant.

Conservation of energy.

We want to construct a microscopic energy density $\epsilon(\mathbf{x})$ whose integral over all of space is the total energy E, which is known from the particle dynamics to be

$$\int \epsilon(\mathbf{x}) = E = \sum_j \frac{m_j}{2}\mathbf{v}_j^2 + U. \tag{4.0.94}$$

Following [26] and [23] we propose a solution which partitions the energy among the particles, assigning ϵ_j to each particle j and then smearing the assigned energy using the ϕ function:

$$\epsilon(\mathbf{x}) = \sum_j \epsilon_j \phi_j \tag{4.0.95}$$

where

$$\epsilon_j = \frac{m_j}{2}\mathbf{v}_j^2 + U^{(j)} \tag{4.0.96}$$

with $\phi_j = \phi(\mathbf{x} - \mathbf{x}_j)$. That is, we assign to each particle its kinetic energy plus some part $U^{(j)}$ of the potential energy where

$$\sum_j U^{(j)} = U. \tag{4.0.97}$$

We demand that $U^{(j)}$ depend only on the particle coordinates $\mathbf{x}_1, \mathbf{x}_2, \cdots$ and so ϵ_j is independent of spatial coordinates. Then the requirement (4.0.94) follows from (4.0.57). We also require that the partitions $U^{(j)}$ satisfy the same invariance principles that U satisfies (translational, rotational, and reflection invariance). Otherwise the partition is arbitrary, and we will see that, although reasonable choices for the partitioning are possible, the arbitrariness will remain. This arbitrariness was pointed out originally by [26, 20].

The insight from [26] is that since we know everything in the conservation equation (4.0.9) except the heat flux $\mathbf{q}$, we use the equation to determine the microscopic form for the heat flux (up to a vector which is divergence-free). But we do not know yet that the proposed energy density

even obeys an equation such as (4.0.9), and the first objective of the following derivation will be to show that this can indeed be done.

Taking the partial derivative of ϵ with respect to time, we get

$$\frac{\partial \epsilon}{\partial t} = \sum_j \epsilon_j \frac{\partial \phi_j}{\partial t} + \sum_j \frac{\partial \epsilon_j}{\partial t} \phi_j \tag{4.0.98}$$

where we can use (4.0.61) to get

$$\frac{\partial \epsilon}{\partial t} = -\frac{\partial}{\partial \mathbf{x}^\mu} \left(\sum_j \mathbf{v}_j^\mu \epsilon_j \phi_j \right) + \sum_j \frac{\partial \epsilon_j}{\partial t} \phi_j \tag{4.0.99}$$

or

$$\frac{\partial \epsilon}{\partial t} = -\frac{\partial}{\partial \mathbf{x}^\mu} \left(\mathbf{v}^\mu \sum_j \epsilon_j \phi_j \right) - \frac{\partial}{\partial \mathbf{x}^\mu} \left(\sum_j \mathbf{u}_j^\mu \epsilon_j \phi_j \right) + \sum_j \frac{\partial \epsilon_j}{\partial t} \phi_j \tag{4.0.100}$$

using the decomposition of particle velocity $\mathbf{v}_j$ into the material velocity $\mathbf{v}$ plus the relative (local) particle velocity $\mathbf{u}_j$. Then

$$\frac{\partial \epsilon}{\partial t} + \frac{\partial}{\partial \mathbf{x}^\mu} \left(\mathbf{v}^\mu \epsilon \right) = -\frac{\partial}{\partial \mathbf{x}^\mu} \left(\sum_j \mathbf{u}_j^\mu \epsilon_j \phi_j \right) + \sum_j \frac{\partial \epsilon_j}{\partial t} \phi_j \tag{4.0.101}$$

We now consider the first term, which is the gradient of

$$\sum_j \mathbf{u}_j^\mu \left(\frac{m_j}{2} \mathbf{v}_j^2 + U^{(j)} \right) \phi_j \tag{4.0.102}$$

and we can rewrite this in terms of relative particle velocities. (4.0.102) becomes

$$\sum_j \mathbf{u}_j^\mu \left(\frac{m_j}{2} \mathbf{u}_j^2 + U^{(j)} \right) \phi_j + \mathbf{v}^\nu \sum_j m_j \mathbf{u}_j^\nu \mathbf{u}_j^\mu \phi_j \tag{4.0.103}$$

where we note that the term proportional to $\mathbf{v}^2$ must vanish, see (4.0.69). Using the expression derived previously for the kinetic part of the stress, and defining the kinetic part of the heat flux as

$$\mathbf{q}_{\mathrm{K}} = \sum_j \mathbf{u}_j^\mu \left(\frac{m_j}{2} \mathbf{u}_j^2 + U^{(j)} \right) \phi_j \tag{4.0.104}$$

we have obtained an analysis of the energy equation for the kinetic parts

$$\frac{\partial \epsilon}{\partial t} + \frac{\partial}{\partial \mathbf{x}^\mu} \left(\mathbf{v}^\mu \epsilon \right) = \frac{\partial}{\partial \mathbf{x}^\mu} \left(\mathbf{v}^\nu \boldsymbol{\sigma}_{\mathrm{K}}^{\mu\nu} - \mathbf{q}_{\mathrm{K}}^\mu \right) + \sum_j \frac{\partial \epsilon_j}{\partial t} \phi_j \tag{4.0.105}$$

We use Hardy's [23] terminology for the separate parts of the heat flux.

Now consider the remaining term

$$\sum_j \frac{\partial \epsilon_j}{\partial t} \phi_j \tag{4.0.106}$$

which can be expanded into

$$\sum_j \left(m_j \mathbf{v}_j^\nu \frac{\partial \mathbf{v}_j^\nu}{\partial t} + \sum_k \mathbf{v}_k^\nu \frac{\partial U^{(j)}}{\partial \mathbf{x}_k^\nu} \right) \phi_j \tag{4.0.107}$$

and using the equations of motion we get

$$\sum_j \left(-\mathbf{v}_j^\nu \frac{\partial U}{\partial \mathbf{x}_j^\nu} + \sum_k \mathbf{v}_k^\nu \frac{\partial U^{(j)}}{\partial \mathbf{x}_k^\nu} \right) \phi_j \tag{4.0.108}$$

Using the partitioning of U and relabelling we thus obtain

$$\sum_j \frac{\partial \epsilon_j}{\partial t} \phi_j = \sum_{jk} \mathbf{v}_k^\nu \frac{\partial U^{(j)}}{\partial \mathbf{x}_k^\nu} (\phi_j - \phi_k) \tag{4.0.109}$$

We can now use the property (4.0.82) of the bond function β_{jk} to write (4.0.106) as the divergence of some quantity:

$$\sum_j \frac{\partial \epsilon_j}{\partial t} \phi_j = -\frac{\partial}{\partial \mathbf{x}^\mu} \left(\sum_{jk} \mathbf{v}_k^\nu \frac{\partial U^{(j)}}{\partial \mathbf{x}_k^\nu} (\mathbf{x}_j^\mu - \mathbf{x}_k^\mu) \beta_{jk} \right) \tag{4.0.110}$$

and at this point we have succeeded in establishing the correct divergence form of (4.0.9).

We can now compute the remaining (potential) part of the heat flux $\mathbf{q}_{\mathrm{R}}$ by satisfying the equation

$$\mathbf{v}^\nu \boldsymbol{\sigma}_{\mathrm{U}}^{\mu\nu} - \mathbf{q}_{\mathrm{R}}^\mu = -\sum_{jk} \mathbf{v}_k^\nu \frac{\partial U^{(j)}}{\partial \mathbf{x}_k^\nu} (\mathbf{x}_j^\mu - \mathbf{x}_k^\mu) \beta_{jk}. \tag{4.0.111}$$

or

$$\mathbf{q}_{\mathrm{R}}^\mu = \mathbf{v}^\nu \boldsymbol{\sigma}_{\mathrm{U}}^{\mu\nu} + \sum_{jk} \mathbf{v}_k^\nu \frac{\partial U^{(j)}}{\partial \mathbf{x}_k^\nu} (\mathbf{x}_j^\mu - \mathbf{x}_k^\mu) \beta_{jk}. \tag{4.0.112}$$

We now split the second term using the decomposition of particle velocities $\mathbf{v}_j$ into material velocity $\mathbf{v}$ and relative particle velocities $\mathbf{u}_j$. Thus

$$\mathbf{q}_{\mathrm{R}}^\mu = \sum_{jk} \mathbf{u}_k^\nu \frac{\partial U^{(j)}}{\partial \mathbf{x}_k^\nu} (\mathbf{x}_j^\mu - \mathbf{x}_k^\mu) \beta_{jk}. + \mathbf{v}^\nu \sum_{jk} \frac{\partial U^{(j)}}{\partial \mathbf{x}_k^\nu} (\mathbf{x}_j^\mu - \mathbf{x}_k^\mu) \beta_{jk} + \mathbf{v}^\nu \boldsymbol{\sigma}_{\mathrm{U}}^{\mu\nu} \tag{4.0.113}$$

The first term we identify as the normal potential heat flux, $\mathbf{q}_{\mathrm{U}}$:

$$\mathbf{q}_{\mathrm{U}}^\mu = \sum_{jk} \mathbf{u}_k^\nu \frac{\partial U^{(j)}}{\partial \mathbf{x}_k^\nu} (\mathbf{x}_j^\mu - \mathbf{x}_k^\mu) \beta_{jk} \tag{4.0.114}$$

and the second term which we call the *churning* heat flux $\mathbf{q}_{\mathrm{C}}$ is given by

$$\begin{aligned} \mathbf{q}_{\mathrm{C}}^\mu &= \mathbf{v}^\nu \left(\boldsymbol{\sigma}_{\mathrm{U}}^{\mu\nu} + \sum_{jk} \frac{\partial U^{(j)}}{\partial \mathbf{x}_k^\nu} (\mathbf{x}_j^\mu - \mathbf{x}_k^\mu) \beta_{jk} \right) \\ &= \mathbf{v}^\nu \mathbf{z}^{\mu\nu} \end{aligned} \tag{4.0.115}$$

defining the churning tensor

$$\mathbf{z}^{\mu\nu} = \boldsymbol{\sigma}_{\mathrm{U}}^{\mu\nu} + \sum_{jk} \frac{\partial U^{(j)}}{\partial \mathbf{x}_k^\nu} (\mathbf{x}_j^\mu - \mathbf{x}_k^\mu) \beta_{jk} \tag{4.0.116}$$

The churning tensor vanishes for pair potentials, using the obvious partitioning. In this case we choose

$$U^{(j)} = \frac{1}{2} \sum_k U_{jk} \tag{4.0.117}$$

where U_{jk} is the pair potential between particles i, j. Then using (4.0.87) we have

$$\mathbf{z}^{\mu\nu} = \frac{1}{2} \sum_{jk} \frac{\partial U_{jk}}{\partial \xi_{jk}} (\mathbf{x}_j - \mathbf{x}_k)^\mu (\mathbf{x}_j - \mathbf{x}_k)^\nu \beta_{jk} + \frac{1}{2} \sum_{ij} \frac{\partial U_{jk}}{\partial \xi_{jk}} (\mathbf{x}_k - \mathbf{x}_j)^\mu (\mathbf{x}_j - \mathbf{x}_k)^\nu \beta_{jk} = 0 \tag{4.0.118}$$

The second property that we can establish for the churning tensor is that its divergence vanishes. Substituting (4.0.77), (4.0.82) into (4.0.116) and taking the divergence, we get

$$\begin{aligned} \frac{\partial \mathbf{z}^{\mu\nu}}{\partial \mathbf{x}^\mu} &= -\sum_j \frac{\partial U}{\partial \mathbf{x}_j^\nu} \phi_j + \sum_{jk} \frac{\partial U^{(j)}}{\partial \mathbf{x}_k^\nu} \frac{\partial}{\partial \mathbf{x}^\mu} (\mathbf{x}_{jk}^\mu \beta_{jk}) \\ &= -\sum_{jk} \frac{\partial U^{(k)}}{\partial \mathbf{x}_j^\nu} \phi_j - \sum_{jk} \frac{\partial U^{(j)}}{\partial \mathbf{x}_k^\nu} (\phi_j - \phi_k) \\ &= -\sum_j \left(\sum_k \frac{\partial U^{(j)}}{\partial \mathbf{x}_k^\nu} \right) \phi_j \\ &= 0 \end{aligned} \tag{4.0.119}$$

where the inner sum must be zero in the last equation because $U^{(j)}$ is invariant under translations. This means that we can write the churning heat source as

$$\frac{\partial \mathbf{q}_{\mathrm{C}}^\mu}{\partial \mathbf{x}^\mu} = \frac{\partial}{\partial \mathbf{x}^\mu} (\mathbf{v}^\nu \mathbf{z}^{\mu\nu}) = \mathbf{z}^{\mu\nu} \frac{\partial \mathbf{v}^\nu}{\partial \mathbf{x}^\mu} \tag{4.0.120}$$

which contains only Galilean invariant terms.

In this derivation we have not made any assumption about reflection invariance or symmetry of the Cauchy stress, so the results so far are valid for general potentials. Using (4.0.85) we write

$$\mathbf{z}^{\mu\nu} = \frac{1}{2} \sum_{jk} G_{jk} \mathbf{x}_{jk}^\nu \mathbf{x}_{jk}^\mu \beta_{jk} + \sum_{jk} \frac{\partial U^{(j)}}{\partial \mathbf{x}_k^\nu} \mathbf{x}_{jk}^\mu \beta_{jk} \tag{4.0.121}$$

and we can introduce a new set of quantities $G_{kp}^{(j)}$ defined by

$$G_{kp}^{(j)} = \frac{\partial U^{(j)}}{\partial \xi_{kp}} \tag{4.0.122}$$

By assumption, the same symmetry properties hold for $U^{(j)}$ that hold for U. Therefore

$$\frac{\partial U^{(j)}}{\partial \mathbf{x}_k^\nu} = \sum_{kp} G_{kp}^{(j)} (\mathbf{x}_k^\nu - \mathbf{x}_p^\nu) \tag{4.0.123}$$

so (4.0.121) can be written as

$$\mathbf{z}^{\mu\nu} = \sum_{jkp} \beta_{jk} \mathbf{x}^{\mu}_{jk} \left(\frac{1}{2} G^{(p)}_{jk} (\mathbf{x}^{\nu}_{j} - \mathbf{x}^{\nu}_{k}) + G^{(j)}_{kp} (\mathbf{x}^{\nu}_{k} - \mathbf{x}^{\nu}_{p}) \right) \tag{4.0.124}$$

To analyze this expression further we need to examine the partition of U. Suppose that U is written in terms of two particle interactions plus three particle interactions and so forth:

$$U = \frac{1}{2} \sum_{jk} U_{jk} + \frac{1}{3} \sum_{jkl} U_{jkl} + \cdots \tag{4.0.125}$$

where we assume that $1/3$ of a three particle interaction term is assigned to each of the participating particles. This is clearly the simplest possible partitioning. For a term that involves K particles we assume that a fraction $1/K$ of the term is assigned to each participating particle.

Since the expression for $\mathbf{z}^{\mu\nu}$ is linear in the potential we can consider each term by itself. We already showed that pair terms will not contribute. Now consider a single term U_t where K particles interact. Then we can write

$$U^{(p)}_{t} = \frac{1}{K} U_t \tag{4.0.126}$$

so that

$$G^{(p)}_{jk} = \frac{1}{K} G^{t}_{jk} \tag{4.0.127}$$

with

$$G^{t}_{jk} = \frac{\partial U_t}{\partial \xi_{jk}} \tag{4.0.128}$$

and this vanishes when j or k is not in the set of K participating particles.

The contribution to the churning tensor from U^t is then

$$\mathbf{z}^{\mu\nu}_{t} = \frac{1}{K} \sum_{jk} \beta_{jk} \mathbf{x}^{\mu}_{jk} \sum_{p} \left(\frac{1}{2} G^{t}_{jk} \mathbf{x}^{\nu}_{jk} + G^{t}_{kp} \mathbf{x}^{\nu}_{kp} \right) \tag{4.0.129}$$

where the sums are taken only over participating particles. Now in the sum over p we treat the terms for $j = p$ and $k = p$ separately, to obtain

$$\begin{aligned} \mathbf{z}^{\mu\nu}_{t} &= \frac{1}{K} \sum_{jk} \beta_{jk} \mathbf{x}^{\mu}_{jk} \left[\frac{1}{2} G^{t}_{jk} \mathbf{x}^{\nu}_{jk} + G^{t}_{kj} \mathbf{x}^{\nu}_{kj} + \frac{1}{2} G^{t}_{jk} \mathbf{x}^{\nu}_{jk} + {\sum_{p}}' \left(\frac{1}{2} G^{t}_{jk} \mathbf{x}^{\nu}_{jk} + G^{t}_{kp} \mathbf{x}^{\nu}_{kp} \right) \right] \\ &= \frac{1}{K} \sum_{jk} \beta_{jk} \mathbf{x}^{\mu}_{jk} {\sum_{p}}' \left(\frac{1}{2} G^{t}_{jk} \mathbf{x}^{\nu}_{jk} + G^{t}_{kp} \mathbf{x}^{\nu}_{kp} \right) \end{aligned} \tag{4.0.130}$$

where ${\sum_{p}}'$ means that terms with $p = j, k$ are excluded from the sum. Now use

$$G^{t}_{kp} \mathbf{x}_{kp} = \frac{1}{2} (G^{t}_{kp} \mathbf{x}_{kp} + G^{t}_{jp} \mathbf{x}_{jp}) + \frac{1}{2} (G^{t}_{kp} \mathbf{x}_{kp} - G^{t}_{jp} \mathbf{x}_{jp}) \tag{4.0.131}$$

to get

$$\mathbf{z}^{\mu\nu}_{t} = \frac{1}{2K} \sum_{jk} \beta_{jk} \mathbf{x}^{\mu}_{jk} {\sum_{p}}' \left(G^{t}_{jk} \mathbf{x}^{\nu}_{jk} + G^{t}_{kp} \mathbf{x}^{\nu}_{kp} - G^{t}_{jp} \mathbf{x}^{\nu}_{jp} \right) \tag{4.0.132}$$

We can repeat the argument that the churning tensor vanishes for pair contributions, since if $K = 2$ then the sum over p has no terms in it.

Further insight into this expression can be obtained by examining the case where $K = 3$. Here we imagine that we have particles a, b, c and we note that $\mathbf{x}_{bc}$ can be written in terms of $\mathbf{x}_{ab}, \mathbf{x}_{ac}$. Doing this we obtain

$$\begin{aligned}\mathbf{z}_t^{\mu\nu} =& \frac{1}{3}\mathbf{x}_{ab}^{\mu}\mathbf{x}_{ab}^{\nu}(G_{ab}^t - G_{bc}^t)(\beta_{ab} - \beta_{bc}) \\ &+ \frac{1}{3}\mathbf{x}_{ac}^{\mu}\mathbf{x}_{ac}^{\nu}(G_{ac}^t - G_{bc}^t)(\beta_{ac} - \beta_{bc}) \\ &+ \frac{1}{3}\mathbf{x}_{ab}^{\mu}\mathbf{x}_{ac}^{\nu}(G_{bc}^t - G_{ac}^t)(\beta_{ab} - \beta_{bc}) \\ &+ \frac{1}{3}\mathbf{x}_{ac}^{\mu}\mathbf{x}_{ab}^{\nu}(G_{bc}^t - G_{ab}^t)(\beta_{ac} - \beta_{bc})\end{aligned} \tag{4.0.133}$$

All of these terms will vanish in the virial limit, where $\beta_{jk} \to 1/V$.

Conjecture: The churning tensor vanishes in the virial limit for arbitrary K. To prove this we would need to show that (4.0.132) only depends on differences of β factors.

The churning tensor does not vanish microscopically. An open question is whether it has any effect on physics; obviously if the conjecture above is true then the effect will vanish at large length scales. Finally, we note that the churning tensor is not symmetric. Therefore it can interact with both the strain rate tensor and the vorticity tensor in the source term (4.0.120) for the energy equation.

Summary.

The mass density field is given by

$$\rho(\mathbf{x}, t) = \sum_j m_j \phi_j \tag{4.0.134}$$

the momentum density is

$$\boldsymbol{\pi}(\mathbf{x}, t) = \sum_j m_j \mathbf{v}_j \phi_j \tag{4.0.135}$$

and the material velocity field is determined to be

$$\mathbf{v}(\mathbf{x}, t) = \frac{\sum_j m_j \mathbf{v}_j \phi_j}{\sum_j m_j \phi_j}. \tag{4.0.136}$$

From the particle dynamics we deduce the stress field

$$\boldsymbol{\sigma}^{\mu\nu}(\mathbf{x}, t) = -\sum_j m_j \mathbf{u}_j^{\mu}\mathbf{u}_j^{\nu}\phi_j - \frac{1}{2}\sum_{jk} \mathbf{f}_{jk}^{\nu}\mathbf{x}_{jk}^{\mu}\beta_{jk} \tag{4.0.137}$$

where the pair force $\mathbf{f}_{jk}$ is given by

$$\mathbf{f}_{jk} = -\mathbf{x}_{jk} G_{jk} \tag{4.0.138}$$

and β_{jk} is Hardy's bond function.

Total and internal energy densities require a partitioning of the potential U. The total energy density is then

$$\hat{\epsilon}(\mathbf{x},t) = \sum_j \left(\frac{1}{2} m_j \mathbf{v}_j^2 + U^{(j)} \right) \delta(\mathbf{x} - \mathbf{x}_j) \tag{4.0.139}$$

and we deduce that the microscopic heat flux is

$$\mathbf{q} = \mathbf{q}_{\mathrm{K}} + \mathbf{q}_{\mathrm{U}} \tag{4.0.140}$$

where the kinetic part of the heat flux is

$$\mathbf{q}_{\mathrm{K}} = \sum_j \mathbf{u}_j^\mu \left(\frac{m_j}{2} \mathbf{u}_j^2 + U^{(j)} \right) \phi_j \tag{4.0.141}$$

and the potential part is

$$\mathbf{q}_{\mathrm{U}}^\mu = \sum_{jk} \mathbf{u}_k^\nu \frac{\partial U^{(j)}}{\partial \mathbf{x}_k^\nu} (\mathbf{x}_j^\mu - \mathbf{x}_k^\mu) \beta_{jk}. \tag{4.0.142}$$

In addition to these two terms there is a churning heat source given by

$$\tag{4.0.143}$$

Conclusions.

Beginning with a microscopic theory (particle mechanics) we are able to construct all of the partial differential equations of continuum mechanics that describe conservation of mass, momentum, angular momentum, and energy. But we come to some unusual conclusions. First, the concept of "pair force" is not well defined and requires some careful analysis. In particular, the strong form of Newton's third law is a consequence of reflection invariance in the microscopic potential. We concluded that the usual assumption of "material particles" and the transformation to material coordinates is problematic. The usual derivation of balance of angular momentum is invalid for this reason and the common result that symmetry of the Cauchy stress is a result of conservation of angular momentum is also faulty. Instead we show that symmetry of the Cauchy stress is a consequence of reflection invariance of the underlying potential. We are able to deduce a simple formula for Cauchy stress in terms of derivatives of the potential with respect to pair distances (or distance parameters); these derivatives form a definition of pair forces that are guaranteed to satisfy the strong form of Newton's third law.

Carrying this argument forward to the energy balance equation we are able to establish microscopic formulas for energy density and heat flux. But these formulas depend on a decomposition of the energy (assignment to particles) which, as other authors have pointed out, is arbitrary. We also show that the energy balance equation has a new term (churning heat source) which does not appear for pair potentials. This term may vanish in the virial limit, which makes its physical impact small.

Formulas for distance parameter representations.

Here we include some simple formulas for distance parameter representation of common multi-body terms.

Let $\mathbf{x}_1, \mathbf{x}_2, \mathbf{x}_3, \mathbf{x}_4$ be four position vectors. We can write the dot product

$$(\mathbf{x}_1 - \mathbf{x}_2) \cdot (\mathbf{x}_3 - \mathbf{x}_4) = \xi_{14} - \xi_{13} + \xi_{23} - \xi_{24}, \tag{4.0.144}$$

which we can easily establish by expanding each of the distance parameters ξ_{ij}. A simpler version of this for three particles is

$$(\mathbf{x}_1 - \mathbf{x}_3) \cdot (\mathbf{x}_2 - \mathbf{x}_3) = \xi_{13} + \xi_{23} - \xi_{12}. \tag{4.0.145}$$

For the cosine of a bond angle θ_{123} between $\mathbf{x}_1 - \mathbf{x}_3$ and $\mathbf{x}_2 - \mathbf{x}_3$ we have

$$\cos\theta = \frac{(\mathbf{x}_1 - \mathbf{x}_3) \cdot (\mathbf{x}_2 - \mathbf{x}_3)}{|\mathbf{x}_1 - \mathbf{x}_3|\,|\mathbf{x}_2 - \mathbf{x}_3|}$$

and using the dot product formula above we get cosine of the bond angle in distance parameter form:

$$\cos\theta_{123} = \frac{\xi_{13} + \xi_{23} - \xi_{12}}{d_{13}d_{23}} \tag{4.0.146}$$

This can be differentiated to obtain

$$\begin{aligned}
\frac{\partial \cos\theta_{123}}{\partial \xi_{12}} &= -\frac{1}{d_{13}d_{23}} \\
\frac{\partial \cos\theta_{123}}{\partial \xi_{13}} &= \frac{1}{d_{13}d_{23}} - \frac{\cos\theta_{123}}{2\xi_{13}} = \frac{1}{d_{13}d_{23}} - \frac{\cos\theta_{123}}{d_{13}^2} \\
\frac{\partial \cos\theta_{123}}{\partial \xi_{23}} &= \frac{1}{d_{13}d_{23}} - \frac{\cos\theta_{123}}{2\xi_{23}} = \frac{1}{d_{13}d_{23}} - \frac{\cos\theta_{123}}{d_{23}^2}
\end{aligned} \tag{4.0.147}$$

For torsion or dihedral angles we can suppose that we want to compute the torsion angle around the bond $\mathbf{x}_2, \mathbf{x}_3$ which is the angle between the plane containing the points $\mathbf{x}_1, \mathbf{x}_2, \mathbf{x}_3$ and the plane containing $\mathbf{x}_2, \mathbf{x}_3, \mathbf{x}_4$. The cosine of this angle is obviously

$$\cos\phi = \frac{((\mathbf{x}_1 - \mathbf{x}_2) \times (\mathbf{x}_1 - \mathbf{x}_3)) \cdot ((\mathbf{x}_4 - \mathbf{x}_2) \times (\mathbf{x}_4 - \mathbf{x}_3))}{|\mathbf{x}_1 - \mathbf{x}_2|\,|\mathbf{x}_1 - \mathbf{x}_3|\,|\mathbf{x}_4 - \mathbf{x}_2|\,|\mathbf{x}_4 - \mathbf{x}_3|} \tag{4.0.148}$$

and after simplification

$$\cos\phi = \frac{\xi_{12}(\xi_{34} - \xi_{24} + \xi_{23}) + \xi_{13}(\xi_{24} - \xi_{34} + \xi_{23}) - \xi_{23}^2}{d_{12}d_{13}d_{24}d_{34}} \tag{4.0.149}$$

Note that $\sin\phi$ is *not* invariant under reflection, so it cannot be computed in the distance parameter representation. Therefore potential terms proportional to something like $cos(n\phi + \delta)$ where δ is a phase factor parameter are not generally invariant under reflection. However, many commonly used potential parameterizations only use torsion phases that are 0 or π and so this problem does not occur.

We can imagine potentials which depend on the area of a triangle defined by three atoms or the volume of a tetrahedron defined by four atoms. For the unsigned area of a triangle one can use Herod's classical formula, and implicitly we see that there must be such a formula for the unsigned volume of a tetrahedron. In fact this is given by the formula of Piero della Francesca.

These formulas are sufficient to transform most standard molecular dynamics potentials into the distance parameter representation. With the above caveat about torsion potentials the stress and force state formulas derived in this paper should be applicable to multibody force fields such as CHARMM [39] and Amber [8]. As another example, the well-known Stillinger-Weber [59] potential for silicon is given as a sum of two body terms and three body terms

$$U = \frac{1}{2}\sum_{ij} f(d_{ij}) + \sum_{i,j,k} g(d_{ij})g(d_{ik})\left(\cos\theta_{ijk} - \frac{1}{3}\right)^2 \tag{4.0.150}$$

where f, g are specified functions. Therefore in distance-parameter form the Stillinger-Weber potential is given by

$$U = \frac{1}{2}\sum_{ij} f(2\sqrt{\xi_{ij}}) + \sum_{i,j,k} g(2\sqrt{\xi_{ij}})g(2\sqrt{\xi_{ik}})\left(\frac{\xi_{ij} + \xi_{ik} - \xi_{jk}}{2\sqrt{\xi_{ij}\xi_{ik}}} - \frac{1}{3}\right)^2. \tag{4.0.151}$$

Given these formulas the generalized forces G_{ij} are computed by simple differentiation using (4.0.40).

Pair forces for the Stillinger-Weber potential.

The Stillinger-Weber potential [59] is a molecular dynamics potential that contains two and three particle terms. The three particle term defining an interaction between particle 1 that is at the center of the interaction and particles 2,3 that form the two bonds is written in terms of the distances d_{12} and d_{13} and the cosine of the angle between the vectors $\mathbf{x}_1 - \mathbf{x}_2$, $\mathbf{x}_1 - \mathbf{x}_3$:

$$h_{123} = \lambda f(d_{12})f(d_{13})\left(\cos\theta_{231} + \frac{1}{3}\right)^2 \tag{4.0.152}$$

where

$$f(x) = \exp\left(\frac{\gamma}{x-a}\right) \tag{4.0.153}$$

The generalized forces can be computed easily using (4.0.147) to obtain

$$\begin{aligned} G_{12} &= \left(-\frac{\gamma}{d_{12}(d_{12}-a)^2} + A_{12}\right)h_{123} \\ G_{13} &= \left(-\frac{\gamma}{d_{13}(d_{13}-a)^2} + A_{13}\right)h_{123} \\ G_{23} &= A_{23}h_{123} \end{aligned} \tag{4.0.154}$$

where

$$
\begin{aligned}
A_{12} &= \frac{2}{\cos\theta_{231} + \frac{1}{3}} \left(\frac{1}{d_{12} d_{13}} - \frac{\cos\theta_{231}}{d_{12}^2} \right) \\
A_{13} &= \frac{2}{\cos\theta_{231} + \frac{1}{3}} \left(\frac{1}{d_{12} d_{13}} - \frac{\cos\theta_{231}}{d_{13}^2} \right) \\
A_{23} &= -\frac{2}{\cos\theta_{231} + \frac{1}{3}} \left(\frac{1}{d_{12} d_{13}} \right)
\end{aligned}
\tag{4.0.155}
$$

Then we have $\mathbf{f}_{12} = -\mathbf{x}_{12} G_{12}$, etc.

References

[1] N. Alibaud and B. Andreianov. Non-uniqueness of weak solutions for the fractal Burgers equation. *Annal. Inst. H. Poincare C: Non-Linear Analysis*, 27:997–1016, 2010.

[2] N. Alibaud, C. Imbert, and G. Karch. Asymptotic properties of entropy solutions to fractal Burgers equation. *SIAM J. Math. Anal.*, 42:354–376, 2010.

[3] B. M. Axelrod and E. Teller. *J. Chem. Phys.*, 11:299, 1943.

[4] G. R. Baker, X. Li, and A. C. Morlet. Analytic structure of two 1D-transport equations with nonlocal fluxes. *Physica D*, 91:349–375, 1996.

[5] U. Balucani and M. Zoppi. *Dynamics of the Liquid State*. Oxford, 1994.

[6] S. Benzoni-Gavage. Local well-posedness of nonlocal Burgers equations. *Diff. Int. Eq.*, 22:303–320, 2009.

[7] J. Biello and J. K. Hunter. Nonlinear hamiltonian waves with constant frequency and surface waves on vorticity discontinuities. *Comm. Pure Appl. Math.*, LXIII:303–336, 2010.

[8] D. Case et al. *J. Comp. Chem.*, 26:1668–1688, 2005.

[9] A. Castro and D. Córdoba. Global existence, singularities and ill-posedness for a nonlocal flux. *Adv. Math.*, 219:1916–1936, 2008.

[10] CEI. EnSight web page. `http://www.ensight.com/`.

[11] A. J. J. Chmaj. Existence of traveling waves for the nonlocal Burgers equation. *Appl. Math. Lett.*, 20:439–444, 2007.

[12] J. D. Cole. On a quasi-linear parabolic equation occurring in aerodynamics. *Quart. Appl. Math.*, 9:225–236, 1951.

[13] C. M. Dafermos. *Hyperbolic Conservation Laws in Continuum Physics*. Springer-Verlag, Heidelberg, 2005.

[14] J. Deslippe, R. Tedstrom, M. S. Daw, D. Chrzan, T. Neeraj, and M. Mills. Dynamic scaling in a simple one-dimensional model of dislocation activity. *Phil. Mag.*, 84:2445–2454, 2004.

[15] J. Droniou. Fractal conservation laws: Global smooth solutions and vanishing regularization. *Prog. Nonlin. Diff. Eq. Appl.*, 63:235–242, 2005.

[16] R. Duan, K. Fellner, and C. J. Zhu. Energy method for multi-dimensional balance laws with non-local dissipation. *J. Math. Pures Appl.*, 93:572–598, 2010.

[17] E. Emmrich and O. Weckner. On the well-posedness of the linear peridynamic model and its convergence towards the Navier equation of linear elasticity. *Commun. Math. Sci.*, 5(4):851–864, 2007.

[18] L. C. Evans. *Partial Differential Equations.* American Mathematical Society, Providence, RI, 1998.

[19] K. Fellner and C. Schmeiser. Burgers-Poisson: A nonlinear dispersive model equation. *SIAM J. Appl. Math.*, 64:1509–1525, 2004.

[20] M. Green. *Journal of Chemical Physics*, 20(4):1281, 1952.

[21] M. Gunzburger and R. B. Lehoucq. A nonlocal vector calculus with application to nonlocal boundary value problems. *Multscale Model. Simul.*, 8:1581–1620, 2010.

[22] J. Hansen and I. McDonald. *Theory of Simple Liquids.* Academic Press, 1976.

[23] R. Hardy. Formulas for determining local properties in molecular-dynamics simulations: Shock waves. *J. Chem. Phys.*, 76(1):622–628, 1982.

[24] E. Hopf. The partial differential equation $u_t + u\,u_x = \mu_{xx}$. *Comm. Pure Appl. Math.*, 3:201–230, 1956.

[25] L. I. Ignat and J. D. Rossi. A nonlocal convection-diffusion equation. *J. Funct. Anal.*, 251:399–437, 2007.

[26] J. H. Irving and J. G. Kirkwood. The statistical mechanical theory of transport processes. IV. the equations of hydrodynamics. *J. Chem. Phys.*, 18(6):817–829, 1950.

[27] F. Kissling, P. LeFloch, and C. Rohde. A kinetic decomposition for singular limits of non-local conservation laws. *J. Diff. Eq.*, 247:3338–3356, 2009.

[28] F. Kissling and C. Rohde. The computation of nonclassical shock waves with a heterogeneous multiscale method. *Networks Hetero. Media*, 5:661–674, 2010.

[29] Kitware Inc. ParaView web page. `http://www.paraview.org/`.

[30] C. Lanczos. *The Variational Principles of Mechanics.* Dover, 1970.

[31] L. Landau and E. Lifshitz. *Mechanics.* Pergamon, 1969.

[32] P. D. Lax. *Hyperbolic Partial Differential Equations.* American Mathematical Society, Providence, RI, 2006.

[33] R. B. Lehoucq and O. A. von Lilienfeld. Translation of Walter Noll's derivation of the fundamental equations of continuum thermodynamics from statistical mechanics. *J. Elast.*, 100:5–24, 2010.

[34] R. J. LeVeque. *Numerical Methods for Conservation Laws.* Birkhäuser, Basel, 1992.

[35] R. J. LeVeque. *Finite Volume Methods for Hyperbolic Problems.* Cambridge University Press, New York, NY, 2002.

[36] H. L. Liu. Wave breaking in a class of nonlocal dispersive wave equations. *J. Nonlin. Math. Phys.*, 13:441–466, 2006.

[37] Y. Liu, D. Pelinovsky, and A. Sakovich. Wave breaking in the Ostrovsky-Hunter equation. *SIAM J. Math. Anal.*, 42:1967–1985, 2010.

[38] J. D. Logan. Nonlocal advection equations. *Int. J. Math. Edu. Sci. Tech.*, 34:271–277, 2002.

[39] A. MacKerell et al. *The Encyclopedia of Computational Chemistry.* 1998.

[40] Malvern. *Introduction to Continuum Mechanics.*

[41] G. Marc and W. McMillan. The virial theorem. *Advances in Chemical Physics*, 58:209–361, 1985.

[42] R. Menikoff and B. J. Plohr. The Riemann problem for fluid flow of real materials. *Rev. Mod. Phys.*, 61:75–130, 1989.

[43] Y. Muto. *J. Phys. Soc. Jpn.*, 17:629, 1943.

[44] W. Noll. Die Herleitung der Grundgleichungen der Thermomechanik der Kontinua aus der statistischen Mechanik. *J. Rat. Mech. Anal.*, 4:627–646, 1955.

[45] W. Noll. Die herleitung der grundgleichungen der thermomechanik der kontinua aus der statistischen mechanik. *Indiana Univ. Math. J.*, 4(5):627–646, 1955. Original publishing journal was the J. Rational Mech. Anal.

[46] M. L. Parks, R. B. Lehoucq, S. J. Plimpton, and S. A. Silling. Implementing peridynamics within a molecular dynamics code. *Computer Physics Communications*, 179(11):777–783, 2008.

[47] S. J. Plimpton. Pizza.py webpage. `http://www.cs.sandia.gov/~sjplimp/pizza.html`.

[48] S. J. Plimpton. Fast parallel algorithms for short-range molecular dynamics. *J. Comp. Phys.*, 117:1–19, 1995. Available at `http://lammps.sandia.gov`.

[49] C. Rohde. Scalar conservation laws with mixed local and nonlocal diffusion-dispersion terms. *SIAM J. Math. Anal.*, 37:103–129, 2005.

[50] P. Seleson and M. Parks. On the role of the influence function in the peridynamic theory. *Int. J. Mult. Comp. Eng.*, 2010. Submitted.

[51] S. Silling and R. B. Lehoucq. Peridynamic Theory of Solid Mechanics. Technical Report SAND 2010-1233J, Sandia National Laboratories, 2010. to appear in Adv. Appl. Mech.

[52] S. A. Silling. Reformulation of elasticity theory for discontinuities and long-range forces. *Journal of the Mechanics and Physics of Solids*, 48:175–209, 2000.

[53] S. A. Silling. Personal communication, 2007.

[54] S. A. Silling and E. Askari. A meshfree method based on the peridynamic model of solid mechanics. *Computer and Structures*, 83:1526–1535, 2005.

[55] S. A. Silling, M. Epton, O. Weckner, J. Xu, and E. Askari. Peridynamic states and constitutive modeling. *J. Elasticity*, 88:151–184, 2007.

[56] P. M. Skinis. Some properties of fractional Burgers equation. *Math. Model. Anal.*, 7:151–158, 2002.

[57] J. Smoler. *Shock Waves and Reaction-Diffusion Equations.* Springer-Verlag, New York, NY, 1994.

[58] M. Snir, S. Otto, S. Huss-Lederman, D. Walker, and J. Dongarra. *MPI: The Complete Reference*, volume 1. The MIT Press, Cambridge, MA., 2 edition, 1998.

[59] F. Stillinger and T. Weber. *Physical Review B*, 31(8):5262, 1985.

[60] P. Thompson. *Compressible-Fluid Dynamics*. McGraw-Hill, New York, NY, 1972.

[61] J. A. Trangenstein. *Numerical Methods for Hyperbolic Partial Differential Equations*. Cambridge University Press, Cambridge, UK, 2007.

[62] D. H. Tsai. *J. Chem. Phys*, 70:1375, 1979.

[63] A. Veksler and Y. Zarmi. Traveling wave solutions of a simple non-local Burgers-like equation, 2002. arXiv:nlin/0207014v1.

[64] A. Veksler and Y. Zarmi. On spatially non-local Burgers-like dynamical systems. *Nonlinearity*, 16:1367–1380, 2003.

[65] G. B. Whitham. *Linear and Nonlinear Waves*. John Wiley & Sons, New York, NY, 1974.

[66] W. A. Woyczyński. *Burgers-KPZ Turbulence*, volume 1700 of *Lecture Notes in Mathematics*. Springer-Verlag, Berlin, 1998.

DISTRIBUTION:

1	MS 1322	John Aidun, 1435
1	MS 0378	Jim Kamm, 1431
1	MS 1320	Rich Lehoucq, 1414
1	MS 1320	Mike Parks, 1414
1	MS 1322	Mark Sears, 1435
1	MS 1322	Stewart Silling, 1435
1	MS 9018	Central Technical Files, 8940-2
2	MS 0899	Technical Library, 4916
2	MS 0619	Review & Approval Desk, 4916
3	MS 0161	Patent and Licensing Office, 4916

Sandia National Laboratories